Received: 1 July 2022 | Revised: 5 December 2022 | Accepted: 12 December 2022

DOI: 10.1111/bre.12744

Basin Research | IAS EAGE | WILEY

RESEARCH ARTICLE

Late Jurassic back-arc extension in the Neuquén Basin (37°S): Insights from structural, sedimentological and provenance analyses

Eliana Acevedo[1] | **Lucía Fernández Paz**[1,2] | **Alfonso Encinas**[3] | **Brian K. Horton**[4] | **Agustín Hernando**[2] | **Victor Valencia**[5] | **Andrés Folguera**[1,2]

[1]Instituto de Estudios Andinos "Don Pablo Groeber" (IDEAN), CONICET-Universidad de Buenos Aires, Buenos Aires, Argentina

[2]Facultad de Ciencias Exactas y Naturales, Universidad de Buenos Aires, Buenos Aires, Argentina

[3]Departamento de Ciencias de la Tierra, Facultad de Ciencias Químicas, Universidad de Concepción, Concepción, Chile

[4]Department of Geological Sciences and Institute for Geophysics, Jackson School of Geosciences, University of Texas at Austin, Austin, Texas, USA

[5]School of the Environment, Washington State University, Pullman, Washington, USA

Correspondence
Eliana Acevedo, Instituto de Estudios Andinos "Don Pablo Groeber" (IDEAN), CONICET-Universidad de Buenos Aires, Buenos Aires, Argentina.
Email: elianabacevedo@gmail.com

Funding information
Agencia Nacional de Promoción Científica y Tecnológica, Grant/Award Number: PICT-2019-00974; Consejo Nacional de Investigaciones Científicas y Técnicas, Grant/Award Number: PUE 22920160100051 and PIP 11220150100426CO; Fondo Nacional de Desarrollo Científico y Tecnológico, Grant/Award Number: 1200428; National Science Foundation, Grant/Award Number: EAR-1918541; Secretaría de Ciencia y Técnica, Universidad de Buenos Aires, Grant/Award Number: 20020150100166BA

Abstract

The Middle Jurassic–Early Cretaceous evolution of the Neuquén Basin is traditionally attributed to a long phase of thermal subsidence. However, recent works have challenged this model. In view of this, we study the Late Jurassic Tordillo Formation, a non-marine depositional unit that marks a shift to regional regression across the basin. Previous studies propose different causes for this regression, including the growth of the magmatic arc in the west, uplift in the south or extension in the north. We studied the Tordillo Formation in sections located at an intermediate position in the Neuquén Basin, in order to understand the tectonic processes active during sedimentation. We present evidence of normal faulting within the Tordillo Formation and the base of the overlying Vaca Muerta Formation. Some of these faults can be attributed as syndepositional. We characterize the Tordillo Formation as part of a distal fan-playa lake depositional system with a contemporaneous western magmatic arc as the main source of sediment. When compared to the Late Triassic–Early Jurassic NE to NNE-oriented rifting, which marks the opening of the Neuquén Basin, the Late Jurassic extension shows a switch in stress orientation; the latter is orthogonal to the north-trending subduction zone. We interpret this change as a renewed phase of back-arc extension induced by slab rollback along with minor distributed intraplate extension prior to opening of the South Atlantic Ocean.

KEYWORDS

extensional basin, Kimmeridgian, normal faulting, southern Central Andes, Tordillo Formation, U–Pb geochronology

1 | INTRODUCTION

The Mesozoic evolution of the western margin of South America involved the establishment of forearc and retroarc basins that document the geodynamic processes and basin-forming mechanisms that have been active along the Andean subduction margin (Charrier et al., 2015; Horton, 2018; Ramos, 2010). Plate convergence rates and the geometry of the subducted slab play fundamental roles in the upper plate configuration, position of the magmatic arc and governing tectonic regime (Guillaume et al., 2009; Jarrard, 1986; Lallemand et al., 2005). The sedimentary fill of retroarc basins is well exposed in the current fold and thrust belts, along the eastern slope of the Andes, for example, the Austral-Magallanes Basin in the Fuegian Andes, the Salta Rift Basin in the Central Andes or the Medina Basin in the Northern Andes (Gallardo Jara et al., 2019; Grier et al., 1991; Parra et al., 2009).

In the southern Central Andes, the Neuquén Basin accommodates a continuous Upper Triassic to lower Cenozoic stratigraphic record that documents the history of the Andean retroarc zone (Legarreta & Gulisano, 1989). The evolution of the Neuquén Basin is traditionally divided into three main intervals: an initial Late Triassic–Early Jurassic rift stage, a long thermal subsidence period from the Middle Jurassic to Early Cretaceous and a final Late Cretaceous–Cenozoic foreland basin stage that records the initial uplift of the Andes (Howell et al., 2005; Legarreta & Gulisano, 1989).

Although the aforementioned three-stage record has become the standard for Neuquén Basin evolution, the post-rift sedimentary succession contains a series of unconformities that can be attributed to punctuated tectonism (Groeber et al., 1953; Leanza, 2009; Legarreta & Uliana, 1996). The most prominent example is the Araucanian (or intra-Malmic) unconformity, of Kimmeridgian age and local angular nature near the southern basin margin (Figure 1a; Silvestro & Zubiri, 2008; Stipanicic & Rodrigo, 1970; Vergani et al., 1995). This unconformity coincides with a basin-wide regression marked by Kimmeridgian–Tithonian conglomerates, sandstones and mudstones deposited in diverse non-marine environments of the Tordillo Formation in Argentina and the Río Damas Formation in Chile (Klohn, 1960; Stipanicic, 1969). This regression phase paradoxically coincides with a global marine highstand (Haq, 2018).

The Kimmeridgian regression is considered to be tectonically forced. Still, there are different proposed tectonic scenarios: (i) disconnection from the paleo-Pacific ocean by the growth of the magmatic arc along the western basin margin (Ramos, 1985; Spalletti et al., 2008; Spalletti & Veiga, 2007); (ii) uplift along the southern basin margin (Mosquera & Ramos, 2006; Silvestro & Zubiri, 2008; Vergani et al., 1995; Zavala & Freije, 2002); and (iii) a new extensional phase in the northern part of the basin (Acevedo et al., 2020; Charrier et al., 2007; Mescua et al., 2020).

Highlights

- Field evidence of syndepositional extension within the Tordillo Formation.
- The Tordillo Formation records the transition from distal fan to playa lake depositional systems.
- U–Pb age patterns suggest the Late Jurassic magmatism as the main source of sediment.
- Late Triassic–Early Jurassic versus Late Jurassic extension show a shift in the stress orientation.

The complexity that surrounds the Tordillo Formation provides the catalyst for this investigation. We focus our fieldwork on the Cordillera del Viento and Cerro Domuyo areas (Figure 1b), as they offer a compelling location to evaluate potential structural controls on the Tordillo Formation. They are located in an intermediate position between the southern basin margin and the northern portion of the Neuquén Basin. Intra-basinal thickness variations are significant; whereas the Tordillo Formation reaches 800 m in the Cordillera del Viento area, it was not deposited in the Reyes-Cara Cura area, only ca. 50 km to the northeast (Figure 2b).

We performed sedimentological, structural, geochronological and petrographic analyses in order to understand the provenance, palaeogeography and paleotectonic setting of the Tordillo Formation. The integration of our new data with previous works supports our reconstruction of the Late Jurassic Neuquén Basin.

2 | GEOLOGICAL SETTING

The Neuquén Basin, located in the southern Central Andes of Argentina and Chile between 32° and 41°S, is a retroarc basin composed of thousands of metres of marine, non-marine and volcanic deposits that accumulated from the Late Triassic to the Cenozoic (Howell et al., 2005). The basin can be divided into two regions: a western Andean sector and an eastern region referred to as the Neuquén Embayment (Figure 1a). In the west, units are better exposed due to Andean uplift, whereas in the east, they occur mainly in the subsurface and are relatively undeformed.

The study area is located in the western part of the Neuquén Basin, between the Cerro Domuyo and the Neuquén River (ca. 37°S), where the basement and

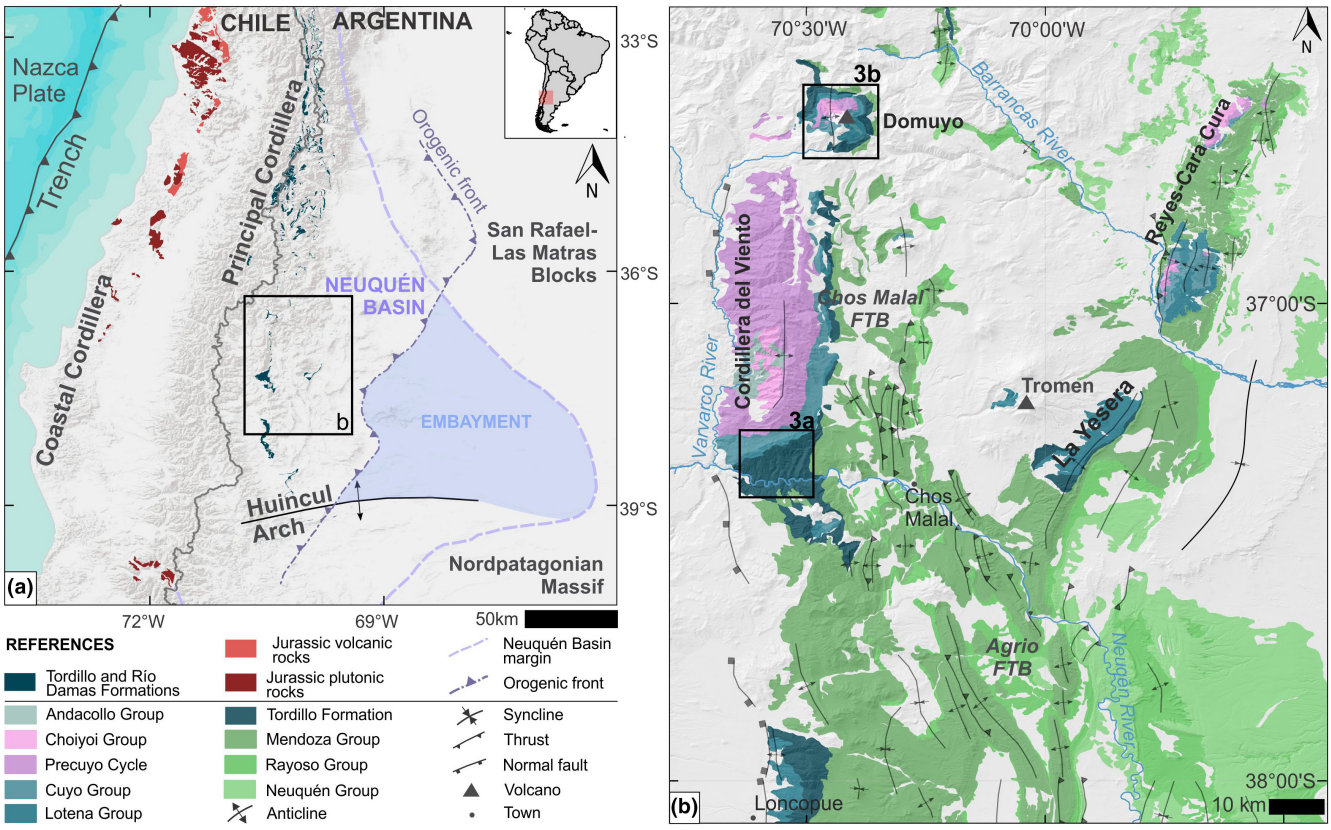

FIGURE 1 (a) Regional map of the southern Central Andes showing the location of the main morphostructural units, the eastern margin of the Neuquén Basin, the orogenic front and outcrop locations of the Jurassic rocks at the Coastal Cordillera and the Tordillo and Rio Damas formations at the Andean axis. (b) Geological map of the study area in an intermediate position of the Neuquén Basin (based on Groeber, 1933; Leanza et al., 2001; Narciso et al., 2004; Ramos, 1981; Rovere et al., 2004; Zöllner & Amos, 1973). Insets show the locations of Figure 3.

sedimentary fill are exposed in the Chos Malal fold and thrust belt, in a complex deformation pattern involving thin- and thick-skinned structures (Folguera et al., 2007; Ramos, 1977; Rojas Vera et al., 2015; Sánchez et al., 2015).

The basement of the Neuquén Basin, exposed by the Chos Malal fold and thrust belt, is composed of metamorphic and igneous rocks of Palaeozoic to Early Triassic age. It is represented by the Upper Devonian–Lower Carboniferous metasedimentary rocks of the Guaraco Norte Formation, Carboniferous pyroclastic and sedimentary rocks of the Andacollo Group, and the Lower Permian-Lower Triassic? Huinganco Complex (Giacosa et al., 2014; Leanza et al., 2005; Zappettini et al., 1987) (Figure 2a). The plutonic member of the Huinganco Complex ranges from granodiorite to monzogranite composition and intrudes the Andacollo Group; the volcanic counterpart consists of dacitic to rhyolitic ignimbrites and subordinated conglomerates and sandstones (Giacosa et al., 2014; Llambías et al., 2007). These rocks record a series of tectonic events that include the accretion of allochthonous terranes, the development of an Andean-type subduction margin along western Gondwana during the late Palaeozoic (Heredia et al., 2018; Ramos et al., 1986) and the establishment of the Choiyoi Magmatic Province—an ensemble of mesosilicic to acid igneous rocks of Permian to Middle Triassic age (Kleiman & Japas, 2009; Llambıas et al., 2003; Sato et al., 2015; Spalletti & Limarino, 2017).

Sedimentation in the Neuquén Basin commenced during the Late Triassic in a series of disconnected depocenters controlled by major NNW to WNW trending normal faults. These faults were activated diachronically from north to south, and their geometries appear to be controlled by Palaeozoic lithospheric weaknesses (Bechis et al., 2010, 2014; D'Elia et al., 2020). The infill of these extensional basins comprises the Precuyo Cycle that includes volcanic, volcaniclastic and non-marine and marine clastic rocks (Bechis et al., 2020; D'Elia et al., 2020; Franzese & Spalletti, 2001; Gulisano, 1993).

By the Early Jurassic, a marine transgression from the paleo-Pacific Ocean connected the previously isolated depocenters, marking the beginning of thermal subsidence in the basin that persisted for ca. 90 m.y. (Vergani et al., 1995;

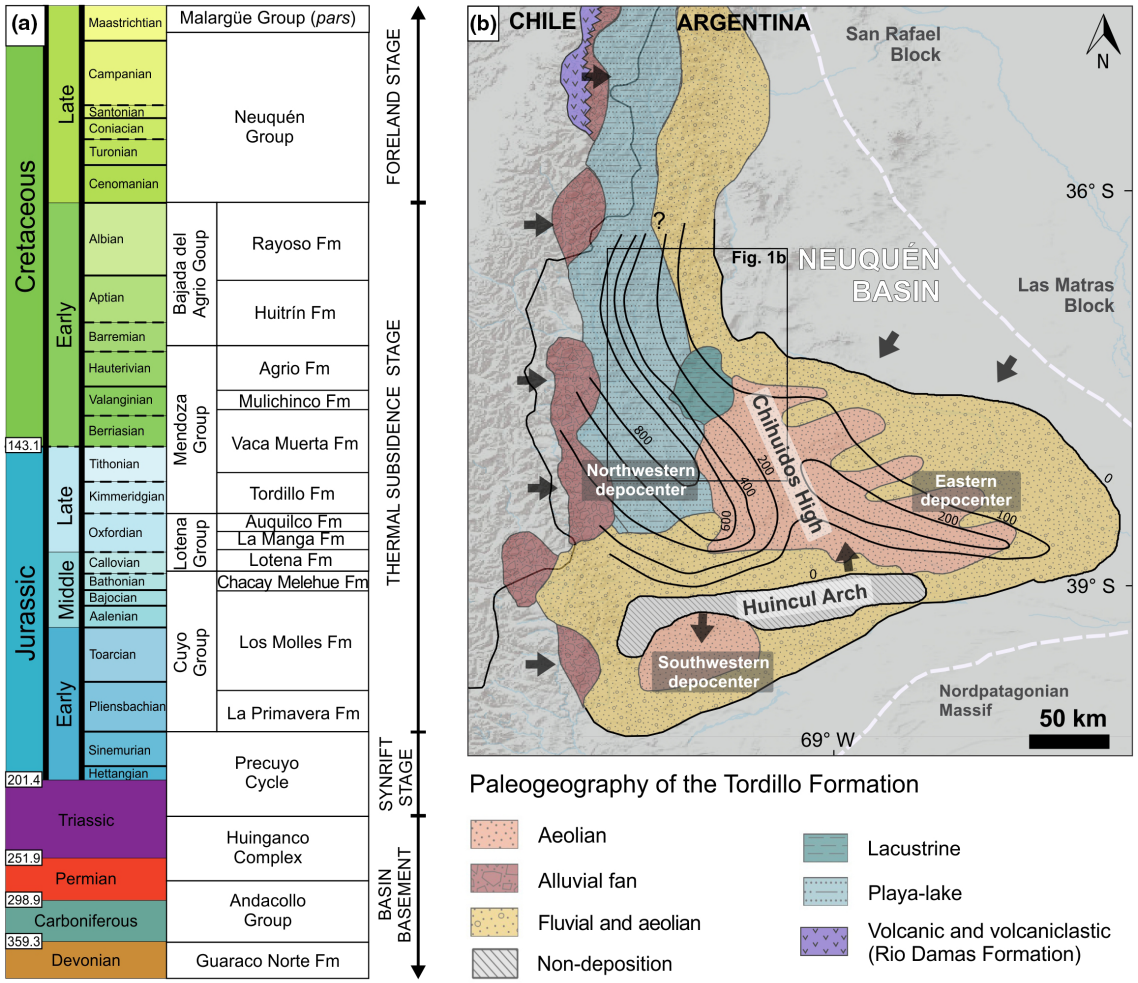

FIGURE 2 (a) Chronostratigraphic chart of the Neuquén Basin and interpreted tectonic stages during basin evolution (from Howell et al., 2005). (b) Late Jurassic facies map of the Neuquén Basin during Tordillo sedimentation. Black arrows show the sediment route direction. Black lines show thickness values (modified from Arregui, 1993; Gulisano, 1988; Spalletti & Veiga, 2007; Spalletti et al., 2011; Vergani et al., 1995).

Vicente, 2005). During this phase, periodic flooding of the basin from the paleo-Pacific Ocean resulted in the accumulation of transgressive–regressive cycles within the Cuyo, Lotena and Mendoza Groups (Figure 2a). Although the Early Jurassic–Early Cretaceous interval is considered tectonically quiescent and dominated by thermal subsidence, there is evidence of brief tectonic activity, particularly in the southern basin margin (Guzmán et al., 2021; Mosquera & Ramos, 2006; Silvestro & Zubiri, 2008; Vergani et al., 1995; Zavala et al., 2020). In addition, based on subsidence analysis, Scivetti and Franzese (2019) propose that only the Cuyo Group (Sinemurian–Middle Callovian) would strictly constitute the post-rift of the Neuquén Basin since Lotena Group sedimentation (Middle Callovian–Late Oxfordian) would have been mainly controlled by dynamic subsidence linked to the subducted slab beneath the western margin of Gondwana.

Since the latest Early Cretaceous, total disconnection from the paleo-Pacific Ocean characterizes the sedimentation in the Neuquén Basin, starting with the evaporitic and epiclastic continental rocks of the Bajada del Agrio Group (Leanza, 2003; Veiga et al., 2005). The final opening of the South Atlantic Ocean gave way to the accelerating westward advance of South America and the tectonic regime became contractional (Russo & Silver, 1996). The extensional back-arc basin transitioned into a retroarc foreland basin (Horton et al., 2016; Mpodozis & Ramos, 1989); Upper Cretaceous synorogenic strata of the Neuquén Group provide the first record of the Andean uplift (Borghi et al., 2019; Di Giulio et al., 2017; Fennell et al., 2017; Tapia et al., 2020; Tunik et al., 2010). Since the Late Cretaceous, the Neuquén Basin registers fluctuations between contractional, neutral and extensional phases during the growth of the Andes (Fennell et al., 2019; Horton & Fuentes, 2016; Ramos & Folguera, 2005).

2.1 | The Late Jurassic Neuquén Basin

During the Late Jurassic, the Neuquén Basin went through a protracted regressive phase that started in the Middle Jurassic with a gradual shoreline retreat to the northwest and peaked by the Kimmeridgian with the complete continentalization of the basin (Vicente, 2006). The Kimmeridgian stage is characterized by non-marine sedimentation of the Tordillo and Rio Damas formations (Figure 2b). The Río Damas Formation, located along the western (Chilean) slope of the Andean axis, contains interbedded volcanic and coarse-grained clastic rocks, with significant thickness variations (Figure 2b) (Klohn, 1960).

The Tordillo Formation, defined on the eastern (Argentinean) side of the Andes, is characterized by the development of alluvial, fluvial, aeolian, playa-lake and lacustrine depositional systems and also presents thickness variations within the Neuquén Basin (Figure 2b). In the southern portion of the basin (36°–41°S), these variations led to the distinction of three main Kimmeridgian depocenters: the northwestern, southwestern and eastern depocenters (Figure 2; Spalletti & Veiga, 2007). The study area is located in the northwestern depocenter where the Tordillo Formation reaches 800 m in thickness (Gulisano, 1988). The depocenter limits are defined by two paleo-highs, the Huincul Arch to the south and the Chihuidos High to the east.

The Huincul Arch, an E-W-oriented structural lineament developed at 39°S (Figure 1a), records intraplate contractional events between the Jurassic and Early Cretaceous (Guzmán et al., 2021; Mosquera & Ramos, 2006; Ploszkiewicz et al., 1984; Silvestro & Zubiri, 2008; Vergani et al., 1995; Zavala et al., 2020). Here, the Tordillo Formation overlies the Lotena and Cuyo Groups in angular unconformity, presents growth-strata wedge geometries or is absent, and it was proposed to be associated with tectonic inversion of pre-existing faults (Freije et al., 2002; Mosquera & Ramos, 2006; Vergani et al., 1995; Zavala et al., 2020; Zavala & Freije, 2002). Provenance studies in the southern sector of the northwestern depocenter show that the Early Jurassic units exhumed at the Huincul Arch deformation zone were an important source of sediment for the Tordillo Formation, along with the coeval Late Jurassic magmatism (Naipauer et al., 2012).

The NW-SE-oriented Chihuidos High (Figure 2b) was a paleo-high during several stages of the basin evolution and also recorded contractional pulses during the Jurassic and Early Cretaceous (Maretto & Pangaro, 2005; Micucci et al., 2018; Mosquera & Ramos, 2006). On the Chihuidos High, the Tordillo Formation reaches a maximum thickness of 200 m (Figure 2; Gulisano, 1988; Spalletti & Veiga, 2007).

North of the Chihuidos High, at the Sierras de Cara Cura and Reyes, the Tordillo Formation was not deposited and the Tithonian-Berriasan Vaca Muerta Formation marine deposits rest unconformably over the Oxfordian Auquilco Formation evaporites (see location in Figure 1b; stratigraphic chart in Figure 2a). This non-depositional

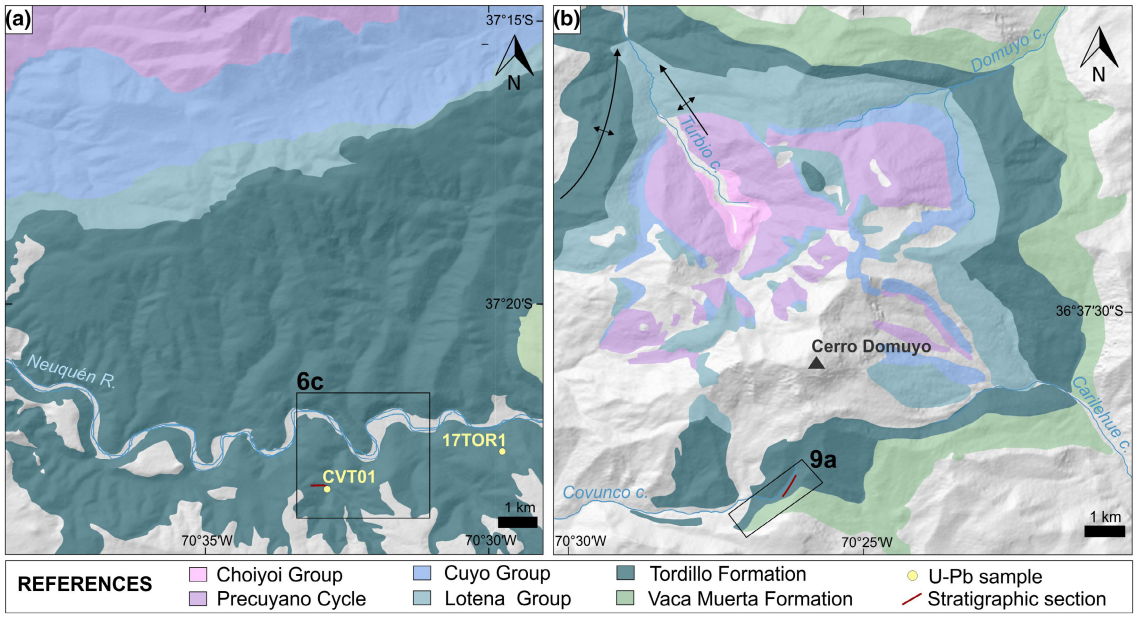

FIGURE 3 (a) Geological map of the Cordillera del Viento area, with the location of the stratigraphic section (Figure 4) and U–Pb samples sites (CVT01 and 17TOR1). The inset shows the location of Figure 6c. (b) Geological map of the Domuyo area showing the location of the studied stratigraphic section (Figure 5). The inset shows the location of Figure 9a.

area of the Tordillo Formation is only 50 km NE from the northwestern depocenter's maximum thickness site.

To the west, Mesozoic units are not exposed since they are covered by the widespread Cenozoic volcanic and volcaniclastic deposits. Therefore, the western limit of the northwestern depocenter, and the Neuquén Basin in general, cannot be defined. Farther north, outcrops of the Tordillo Formation are scarce and the extension of the Late Jurassic northwestern depocenter is uncertain.

In the northern portion of the Neuquén Basin (32°–35°S), the Tordillo Formation shows a systematic increase in thickness and in the volcanic and volcaniclastic material from east to west, as it transitions to the Rio Damas Formation (Acevedo et al., 2020; Lo Forte, 1996; Mescua et al., 2020; Sanguinetti, 1989; Sruoga et al., 2011). At this latitude, the basin has a N-S elongated shape and Tordillo Formation's thickness changes occur rapidly across this narrow segment. In the western sector, the Río Damas Formation achieves thicknesses between 1000 and 5000 m (Charrier, 1981; Davidson, 1988; Klohn, 1960). The Río Damas Formation only crops out in the northern portion of the Basin, on the western margin. South of 36°S, the development of the Río Damas volcanism is unknown due to the extensive development of the Cenozoic units (Figure 2b).

Although the Jurassic magmatic arc was centred along the Coastal Cordillera (Gana & Tosdal, 1996; Vergara et al., 1995), the Late Jurassic Río Damas Formation developed along an eastern magmatic axis ca. 100 km to the east, on the present day Chilean slope of the Principal Cordillera (Figure 1a). The Río Damas Formation igneous rocks have been assigned to subduction-related arc volcanism (Rossel et al., 2014) or retroarc magmatism (Charrier et al., 2007).

U–Pb geochronological analyses on the Tordillo and Río Damas formations show a maximum depositional age between 151 and 143 Ma for these units (Horton et al., 2016; Junkin & Gans, 2019; Naipauer et al., 2012; Naipauer, Tapia, et al., 2015; Naipauer, Tunik, et al., 2015; Rossel et al., 2014). An ash bed located at the top of the Tordillo Formation ca. 50 km east of the study area (La Yesera, Figure 1b) yielded an age of 147.112 ± 0.078 Ma (Lena et al., 2019). These absolute ages fall within the Kimmeridgian (154.8–149.2) and Tithonian (149.2–143.1) stages, according to the GTS2020 (Gradstein et al., 2020). The Tordillo and Río Damas formations calculated ages fall beyond the Kimmeridgian age originally assigned based on stratigraphic relations with fossiliferous marine units. Several studies discuss this discrepancy and its implications for the Jurassic–Cretaceous boundary (Kietzmann et al., 2015; Kietzmann & Martínez, 2018; Lena et al., 2019; Naipauer, Tunik, et al., 2015; Vennari et al., 2014).

By the Tithonian, a new transgression from the paleo-Pacific Ocean flooded the basin, recorded by marine deposits of the Vaca Muerta Formation (and equivalent units) that conformably overlie the Tordillo Formation (Legarreta & Uliana, 1991, 1996).

3 | METHODS

We carried out sedimentological, structural, geochronological and petrographic analyses in the Tordillo Formation within the northwestern depocenter of the Neuquén Basin. In this area, the Tordillo Formation crops out as a N-S strip within the Chos Malal fold and thrust belt, with major exposures at Cerro Domuyo (36° 30′-36° 40′S) and the southern Cordillera del Viento (37° 20′-37° 30′S) (Figures 1b and 3).

We logged two sedimentological sections, one to the south of the Neuquén River at the southern Cordillera del Viento area and another one in the Covunco creek at the Cerro Domuyo area (Figure 3). We selected the location for the Cordillera del Viento section based on outcrop quality and accessibility to observe lateral and vertical variations, near the structural measurement locations. At these locations, the base and top of the Tordillo Formation do not crop out, therefore, the position within the column is unknown. The Cerro Domuyo section was logged at the upper Tordillo Formation, although the uppermost beds were out of reach or covered.

Structural and sedimentary orientation data were systematically measured in the field using the FieldMove Clino mobile app on an iPhone device (Whitmeyer et al., 2019). We measured 89 fault planes in the Cordillera del Viento area. The stress orientation axes for the dataset of fault planes measured were calculated with the linked Bingham statistics function of the Faultkin 8 software (Allmendinger et al., 2012; Marrett & Allmendinger, 1990). Fault plane coordinates and attitude data are available in the Supporting Information.

To constrain the age of deposition and sedimentary provenance of the Tordillo Formation at the Cordillera del Viento area, we collected two sandstone samples (samples CVT01 and 17TOR1; Figure 3a). Sample CVT01 is positioned within the lower sandstone levels of the Cordillera del Viento stratigraphic section (Figure 4). Sample 17TOR1 is located ca. 5 km towards the east in a comparable stratigraphic level, in order to constrain lateral variations in the provenance. Zircon U–Pb age distribution for both the samples were generated by laser ablation inductively coupled plasma mass spectrometry (LA-ICP-MS). Sample CVT-01 was analysed at Zirchron LLC, following operating procedures and parameters from Chang et al. (2006). Sample 17TOR1 was analysed at the

Arizona LaserChron Center following techniques defined by Gehrels et al. (2008) and Gehrels and Pecha (2014). Probability distribution plots for data visualization were created using Isoplot (Ludwig, 2003). Sample coordinates and tabulated U–Pb (LA-ICPMS) data are available in the Supporting Information.

Maximum depositional ages (MDA) were calculated by three different methods: the maximum likelihood age (MLA) algorithm (Vermeesch, 2021); the youngest single grain (YSG); and the youngest graphical peak on the probability density plot (YPP) (Dickinson & Gehrels, 2009). MLA estimates were calculated with IsoplotR (Vermeesch, 2018).

To complement the U–Pb zircon provenance results, we performed petrographic point counts on five sandstone samples from the Tordillo Formation: three samples from the Cordillera del Viento section and two samples from the Cerro Domuyo section (Figures 4 and 5). For each sample, between 300 and 450 grains were counted according to the Gazzi-Dickinson method (Ingersoll et al., 1984) using a microscope mechanical stage and a Swift automatic point counter. Point count data results are available in the Supporting Information.

4 | RESULTS

4.1 | Sedimentological analysis

We logged two stratigraphic sections, one in the Cordillera del Viento area and another in the Cerro Domuyo area, and identified 10 lithofacies for both localities (Table 1; Figures 4 and 5; locations in Figure 3). The Cordillera del Viento section is ca. 90 m thick and is composed of ca. 10 m of sandstones and conglomerates at the basal levels (lithofacies LF1, LF2 and LF3), followed by ca. 10 m of cross-bedded sandstones interbedded with massive and laminated mudstones and fine sandstones (LF2, LF5 and LF6), and ca. 70 m of massive and laminated sandstones and mudstones with recurrent desiccation cracks (LF7, LF9 and LF8). The Cerro Domuyo section is mainly composed of ca. 40 m of interbedded massive sandstones and mudstones, also with periodic desiccation cracks (LF7, LF9 and LF8). It is worth highlighting that the sedimentary rocks of the upper Tordillo Formation present similar characteristics between the Cordillera del Viento and Cerro Domuyo logs. We recognized two facies' associations, based on the interrelations between the lithofacies described in Table 1.

4.1.1 | Facies association1 (FA1): Fluvial channel deposits

FA1 consists of lenticular beds of conglomerates and sandstones between 1 and 10 m thick. Structureless (massive) to crudely bedded clast-supported pebble conglomerates with erosive bases (LF1) commonly define the base of FA1. LF1 passes upwards to granule and sandstones with trough and planar cross-bedding (LF2 and LF3; Figure 4c). These lenticular beds present a fining-upward arrangement and, in some cases, asymmetric ripples (LF4) are preserved on top. In a few locations, this fining-upwards vertical arrangement culminates with mudstones with desiccation cracks (LF8) (Figure 4i,j). Paleocurrents measured from sandstone cross-sets show flow directions between NNW and NE.

FA1 is prevalent in the lower levels of the logged section at the Cordillera del Viento area, interbedded with the Facies association2 (FA2) (Figure 4a). In the lower levels, LF1, LF2 and LF3 are dominant. In the upper levels of the section, LF4 is preserved, LF1 is absent, and FA1 is interbedded with FA2.

4.1.1.1 | *Interpretation*

The grain size, erosive bases, sedimentary structures, fining-upward arrangement and lenticular geometries indicate deposition within a channelized fluvial system (Bridge, 2003; Miall, 1996). Conglomerates and sandstones with trough cross-bedding (LF2) were deposited in 3D dunes. Planar cross-bedded conglomerates and sandstones (LF3) were formed as 2D dunes. The absence of lateral accretion deposits and relative consistency in paleocurrent directions suggest relatively low-sinuosity channels of a braided fluvial system (Bridge, 2003; Ferguson, 1977). The upward-fining vertical arrangement with the preservation of sand ripples suggests a gradual waning in the discharge and eventual abandonment of the channel (Miall, 1977). The occurrence of desiccation cracks indicates subaerial exposure between flood events (Collinson, 1996).

4.1.2 | Facies association 2 (FA2): Unconfined flow deposits

FA2 is composed of laminated or structureless (massive) mudstones (LF5), laminated fine sandstones (LF6) and sporadic sandstone beds with asymmetric ripples (LF4). It also contains alternations of chaotically layered fine sandstones and mudstones (LF7), massive medium to coarse sandstones (LF9) and fine sandstones or mudstones with desiccation cracks (LF8).

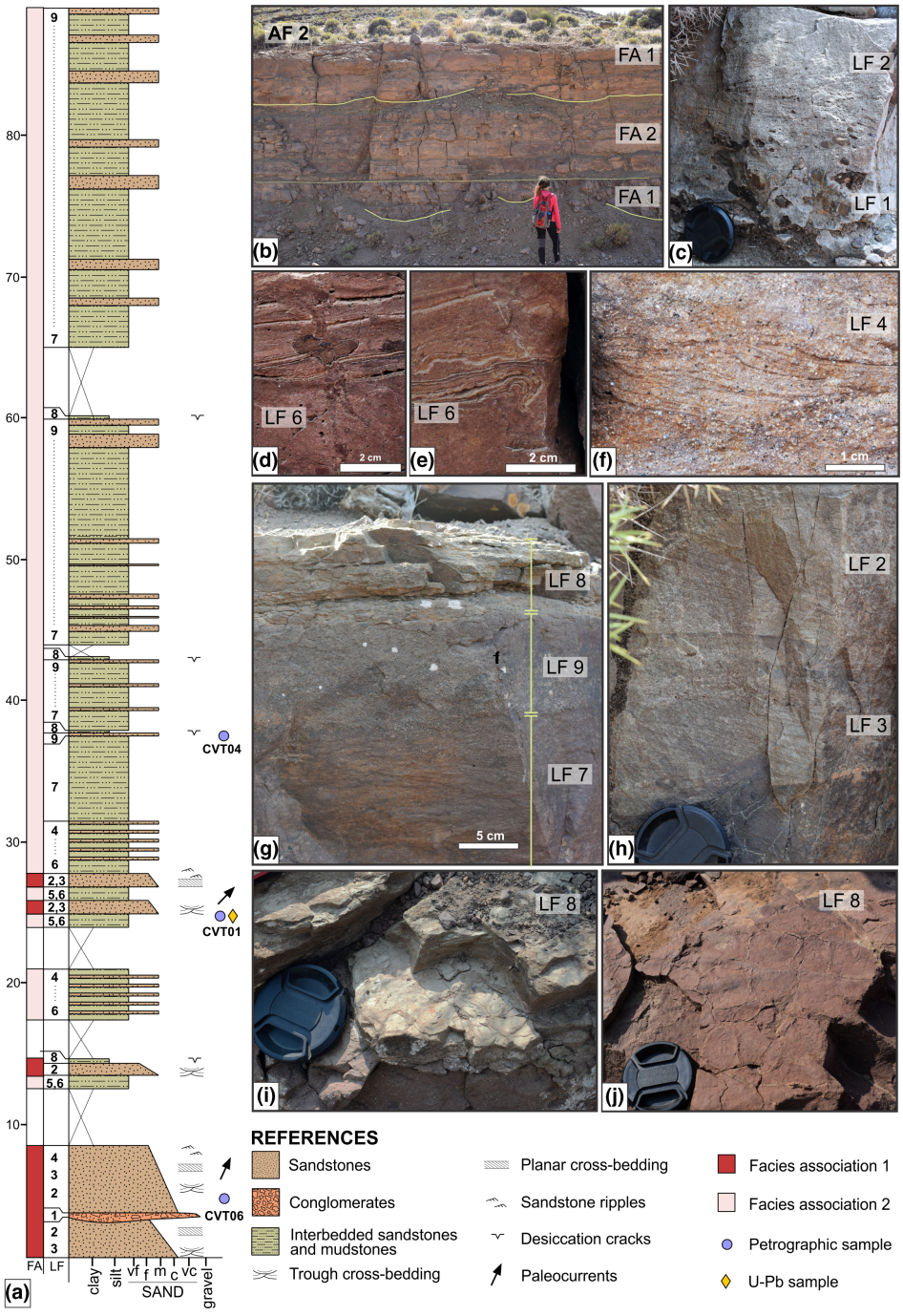

FIGURE 4 (a) Stratigraphic section logged at the Cordillera del Viento area. (b) General view of the lower part of the logged section, with tabular and lenticular beds and interbedded fine and coarse sandstones with erosional contacts. (c) Channel lag defined by upward-fining coarse sandstone with trough cross-bedding and intraclasts up to 4 cm. (d) Small-scale clastic dyke. (e) Convolute lamination. (f) Asymmetric ripples. (g) Planar and trough cross-bedding. (i,j) Desiccation cracks. Lens cap diameter: 5.5 cm. FA, facies association; LF, lithofacies.

The first group (LF5, LF6 and LF4) presents a tabular geometry and is situated in lower levels of the Cordillera del Viento section, interbedded with FA1 (Figure 4b). The thickness of the group varies between 0.5 and 2.5 m. Soft sediment deformation structures are common, including convolute bedding (Figures 4e and 5f), small-scale clastic dykes (Figures 4d and 5g), load casts and flame structures.

The second group (LF7, LF9 and LF8) is dominant in the upper part of the Cordillera del Viento section (Figure 4a) and throughout the Cerro Domuyo section (Figure 5a,c). LF7 forms continuous beds that contain small-scale structures such as ripples, local wavy bedding, dish and pillars, convolute bedding and other soft-sediment deformation structures (Figure 4g). LF7 bed thickness ranges between

0.5 and 6 m. On top of this facies, LF9 typically presents sharp contacts with LF7. Bed thicknesses of LF9 are up to 1 m. Beds with desiccation cracks (LF8) overlie LF9 but are not always present. In some cases, planar laminated sandstones (LF10) and asymmetric ripples (LF4) cap LF7 (Figure 5e).

4.1.2.1 | *Interpretation*

The dominance of fine-grained deposits and the alternation between fine sandstones and mudstones indicates generally lower flow regime conditions, fluctuating between suspension and traction transport mechanisms (Leeder, 1999). The tabular geometry, lower flow regime conditions and absence of lenticular scours or rapid lateral textural variations suggest that FA2 was generated by unconfined flows (Bridge, 2003; Fisher et al., 2007; Miall, 1996). The development of upper flow regime laminated sandstones (LF10) and current ripples (LF4) is associated with the waning stage of the unconfined flows (Tunbridge, 1981). Tabular structureless sandstones (LF9) indicate rapid deposition due to the deceleration of hyperconcentrated flows during unconfinement (Horn et al., 2018). The development of mudstones with desiccation cracks (LF8) indicates flow cessation, the fallout of the suspended load and later exposure to subaerial conditions (Miall, 1977). The recurrence of subaerial exposure suggests that the flows were episodic. The presence of soft-sediment deformation structures can be associated with rapid accumulation rates or potentially seismic events (Allen, 1977; Owen et al., 2011).

4.2 | Structural analysis

Extensional faults cut the Tordillo Formation outcrops in the study area. In the Cordillera del Viento area, along the Neuquén River, the fine-grained composition, tabular geometry and horizontal orientation of the Tordillo beds enable clear identification of multiple structures (Figure 6).

We systematically measured the normal faults that crop out along the southern Cordillera del Viento, principally on the southern side of the Neuquén River (Figure 6c). Due to the horizontal to sub-horizontal nature of the beds in this area, back-tilting corrections were not necessary. The dominant strike values are towards the NW to NNW, with a secondary NE value (Figure 4c). Fault dip angles range from 45° to 89°. A classification by dip angle and the corresponding rose diagrams show different trends for each interval (Figure 6e). Shallowly dipping faults (between 45° and 60°) are scarce ($N = 6$) and E dipping. Faults with a dip angle between 60° and 70° ($N = 15$) present a primary NW to NNW strike (337° to 350° azimuth), where faults dip to the E and W in an apparent conjugate fault system, along with a secondary NW striking group (300° azimuth) with a similar conjugate appearance. The group of steeply dipping faults (between 70° and 80°) also presents a primary NW to NNW strike with E and W dipping directions, with no apparent secondary trend. In the final group of near-vertical faults (over 80° dip), there are two main strike directions: NW to NNW and NE. It is noteworthy that the NE fault trend only appears for the high-angle faults, principally in those dipping >80°. The absence of kinematic indicators in high-angle faults precludes the determination of fault-slip directions.

To complement the measured data, we traced and sketched the normal faults observed in the field and other lineaments observed on satellite images (Figure 6c). These lineaments trend to the NE and the NW, similar to the faults measured in the field.

Most of the observed structures are located on the southern flank of the Neuquén River (Figure 6a). The most conspicuous zone of faulting (Figure 6b) contains several large-scale normal faults and minor associated faults. There is an apparent decrease in fault offset towards upper stratigraphic levels (red lines in Figure 6b). To the east (Figure 6a), Tordillo Formation strata present dip angle variations (Figure 7a). Interestingly, in a closer look, there is a SE dipping normal fault with associated wedge-shaped fine-grained strata (Figure 7b). These strata show an increase in both angle and thickness towards the fault plane, while coarser grained sandstone beds appear discontinuous and lens-shaped. Further to the east (Figure 6a), an E-W vertical section of the Tordillo Formation exposes a series of normal faults with thickness variations of the strata between horst and graben structures (Figure 7c; left) and dip angle variations of the sedimentary beds from 17° to 9° NE (Figure 7c; right).

Outcrops shown in Figure 8 are on opposite slopes of the same creek (Figure 6a), providing 3D constraints of the same structure from different vertical sections. In Figure 8a, a package of tilted strata is associated with a series of normal faults and overlaid by horizontal beds. The relation between these two packages of strata defines onlap and offlap relations and an angular unconformity (Figure 8a; black triangles and red line). Towards the SW, the bed that defines the unconformity appears to be affected by a blind normal fault (Figure 8a; on the centre of the image) and it folds. On top, another unconformity develops (Figure 8a; yellow line). On the opposite slope, there is a similar relation between tilted and horizontal strata, so we infer the position of the unconformity (Figure 8a; dotted red line). Regardless, we interpret that the tilted strata might be linked to a NW dipping normal fault.

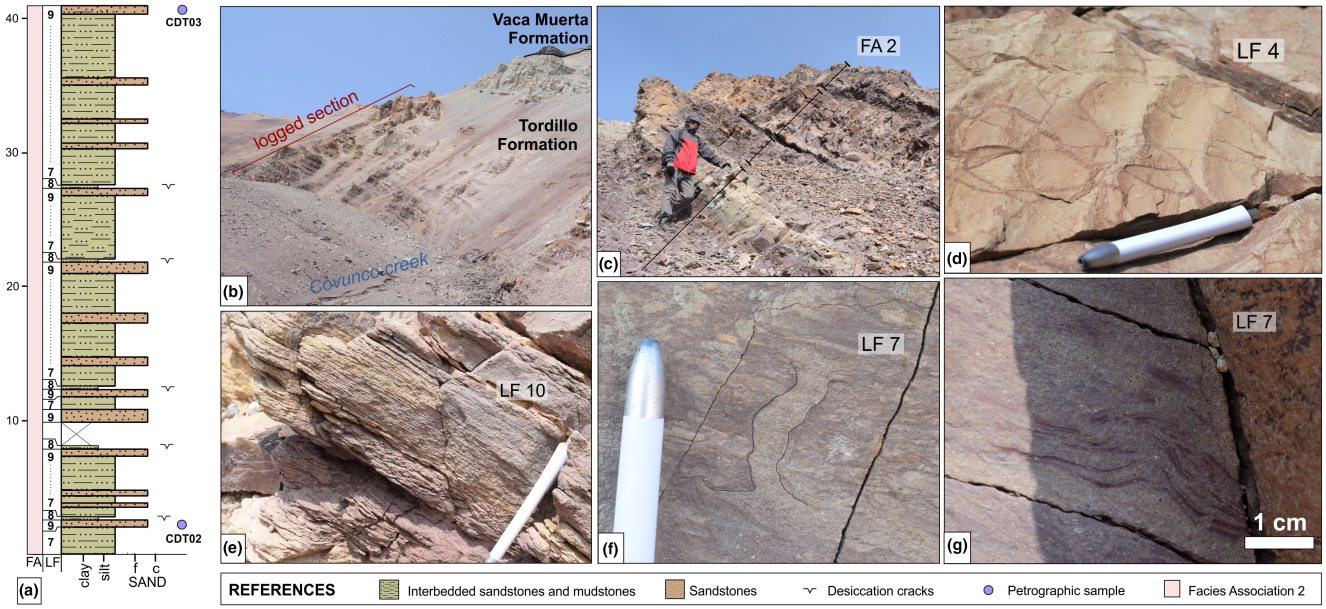

FIGURE 5 (a) Stratigraphic section logged at Cerro Domuyo. (b) General view of the logged section, along the Covunco creek. (c) Cycles from unconfined flow deposits (FA2). (d) Asymmetric ripple marks. (e) Horizontal lamination in sandstones. (f) Small-scale clastic dyke. (g) Convolute lamination. FA, facies association; LF, lithofacies.

North of the Neuquén River, a large SW dipping normal fault presents a rollover anticline structure in the hanging wall, against a footwall that appears deeply fragmented (Figure 7d).

At the Cerro Domuyo area, along the Covunco creek, extensional faults cut the upper Tordillo Formation and reach the base of the Vaca Muerta Formation (Figure 9). These faults were previously described by Kietzmann and Vennari (2013). We noticed an increase in the thickness of the lower section of the Vaca Muerta Formation towards the SW (Figure 9a), accompanied by dip variations within the Tordillo Formation (Figure 9c), potentially linked to a master normal fault located towards the SW.

Based on field measurements of 89 meso- and small-scale normal faults planes at the Cordillera del Viento area, we calculated the stress orientations for Tordillo extensional faults using the Faultkin 8 software (Allmendinger et al., 2012; Marrett & Allmendinger, 1990). The calculated minimum stress vector is oriented in an E-W direction (Figure 6d; axis 1: 092°).

4.3 | U–Pb geochronology

Results for U–Pb analyses of detrital zircon grains are presented for CVT-01 and 17TOR1 samples from Cordillera del Viento. For sample CVT-01, 113 zircon grains were analysed, with three grains discarded due to high discordance. The 110 concordant ages display a multimodal distribution and age range between 143 and 367 Ma. Most zircons are of Jurassic ages, with the main peak at ca. 148 Ma and minor peaks at ca. 157 and 174 Ma (Figure 10a). There is a minor population of Early Permian age (five grains) and a single grain of Late Devonian age.

For sample 17TOR1, 126 zircon grains were analysed, with six grains discarded due to high discordance or analytical error. The 120 concordant ages display a multimodal distribution and range between 143 and 2453 Ma. Most zircons are of Jurassic ages, with the main peak at ca. 152 Ma and minor peaks at ca. 182 and 271 Ma (Figure 10a). There are minor populations of Palaeozoic and Precambrian ages.

Sample CVT01 yielded MDA estimates of 148.69 ± 0.27 Ma (MLA, Vermeesch, 2021), 148 Ma (YPP) and 143.0 ± 1.8 Ma (YSG). Sample 17TOR1 yielded MDA estimates of 151.88 ± 0.32 (MLA, Vermeesch, 2021), 152 Ma (YPP) and 143.56 ± 1.71 Ma (YSG) (Dickinson & Gehrels, 2009).

While the MLA and the YPP methods provide similar results, the YPP method fails to provide an uncertainty value. The YSG method provides a younger MDA for both samples but is not recommended because single data points can exhibit high errors and the effects of lead loss (Coutts et al., 2019). Therefore, we select the MLA results, consistent with previous geochronologic analyses of the Tordillo and Rio Damas formations (Horton et al., 2016; Junkin & Gans, 2019; Naipauer et al., 2012; Naipauer,

TABLE 1 Lithofacies of the Tordillo Formation at the Cerro Domuyo and southern Cordillera del Viento

Lithofacies and sedimentary features	Interpretation
LF1. *Clast supported conglomerates*. Poorly sorted with clast imbrication. Crude bedding and upward-fining internal arrangement. Subangular to subrounded clasts, with a maximum clast size of 4 cm. Bed thickness is up to 15 cm, and geometry is lenticular, with an erosional base. The top is gradational, to LF2	Channel lag deposits
LF2. *Through cross-bedded sandstones and granules*. Clast supported, moderately sorted, with upward-fining arrangement. The base is erosional or transitional from LF1. Local mud intraclasts. Individual cross-sets are 10–30 cm thick. Amalgamated bodies are up to 1.5 m thick. Bed geometry is lenticular to tabular on outcrop scale. Paleoflow directions are towards the NNW, N and NE	Migration of 3D sand dunes
LF3. *Planar cross-bedded sandstones and granules*. Clast supported, moderately sorted. Planar base. Individual cross-sets are up to 15 cm thick. Sets are amalgamated and usually linked to LF2. Paleoflow directions are towards the NNW, N and NE	Migration of 2D sand dunes
LF4. *Fine to medium sandstones with ripples*. Ripple sets are asymmetric and ca. 2 cm thick. Beds thickness is between 15 and 30 cm. This lithofacies caps LF2 and LF3 and underlies LF5	Migration of sand ripples in lower flow regime
LF5. *Structureless (massive) and laminated mudstones*. Tabular geometry. Beds are of centimetre-scale, with intervals up to 50 cm thick. This lithofacies occurs between LF4 and LF6	Mud deposition due to suspension settling in a floodplain environment
LF6. *Laminated fine-grained sandstones*. Dm-scale packages with tabular geometry. Individual beds are up to 2 cm thick. Soft sediment deformation structures: convolute bedding, load casts and flame structures	Episodic sandy sheetfloods, lower flow regime conditions
LF7. *Chaotically layered mudstones and fine sandstones*. Tabular beds, between 0.5 and 6 m thick. Heterolithic alternations of sandstone and mudstone, wavy bedding and ripple-cross bedding. Small lenses with horizontal lamination. Abundant soft-sediment deformation structures: convolute bedding, dish and pillars, load casts and flame structures. The chaotic aspect reflects a combination of depositional and deformational structures	Episodic muddy and sandy sheetfloods, lower and upper flow regime conditions
LF8. *Sandstones and mudstones with desiccation cracks*. This lithofacies occurs occasionally on top of LF9. Individual beds are up to 2 cm thick, with sharp bases and desiccation cracks on top. Stacked beds can reach 10 cm. Mudcracks are polygonal to irregular in plan view, about 1 cm thick, and filled with coarser sand	Dessication after subaerial exposure
LF9. *Structureless (massive) sandstones*. Medium to coarse sandstones, with tabular geometry. Erosive base. Beds are 0.15 to 1 m thick	Rapid deposition of bedload of unconfined flows, during high discharge conditions
LF10. *Planar laminated sandstones*. Tabular beds of sandstones with horizontal laminations, with thicknesses between 5 and 40 cm. Sharp bases	Deposition in upper flow regime, as an unconfined flow

Tapia, et al., 2015; Naipauer, Tunik, et al., 2015; Rossel et al., 2014).

4.4 | Sandstone petrography

The five samples analysed are composed of poorly sorted, medium to coarse sands of sub-rounded to sub-angulose grains. Petrographic analysis reveals that the composition of the sandstones of the Tordillo Formation is lithic feldsarenite to feldspathic litharenites (Folk et al., 1970).

Point count results are plotted on a QFL provenance diagram from Dickinson et al. (1983) (Figure 10b), showing diverse results, indicative of a transitional magmatic arc (samples CDT02 and CDT03 from the Cerro Domuyo, and sample CVT04 from the Cordillera del Viento) and a dissected magmatic arc (samples CVT01 and CVT06 from the Cordillera del Viento).

5 | DISCUSSION

5.1 | Provenance

Detrital zircon U–Pb analyses and sandstone petrographic data are consistent and show main peaks of ca. 148 and 152 Ma (samples CVT01 y 17TOR1 respectively) that suggests contemporaneous magmatism was the main source of sediment for the Tordillo Formation at the Cordillera del Viento and Cerro Domuyo areas (northwestern depocenter of the Neuquén Basin). Late Jurassic magmatic units are located to the west of the basin, included within the Río

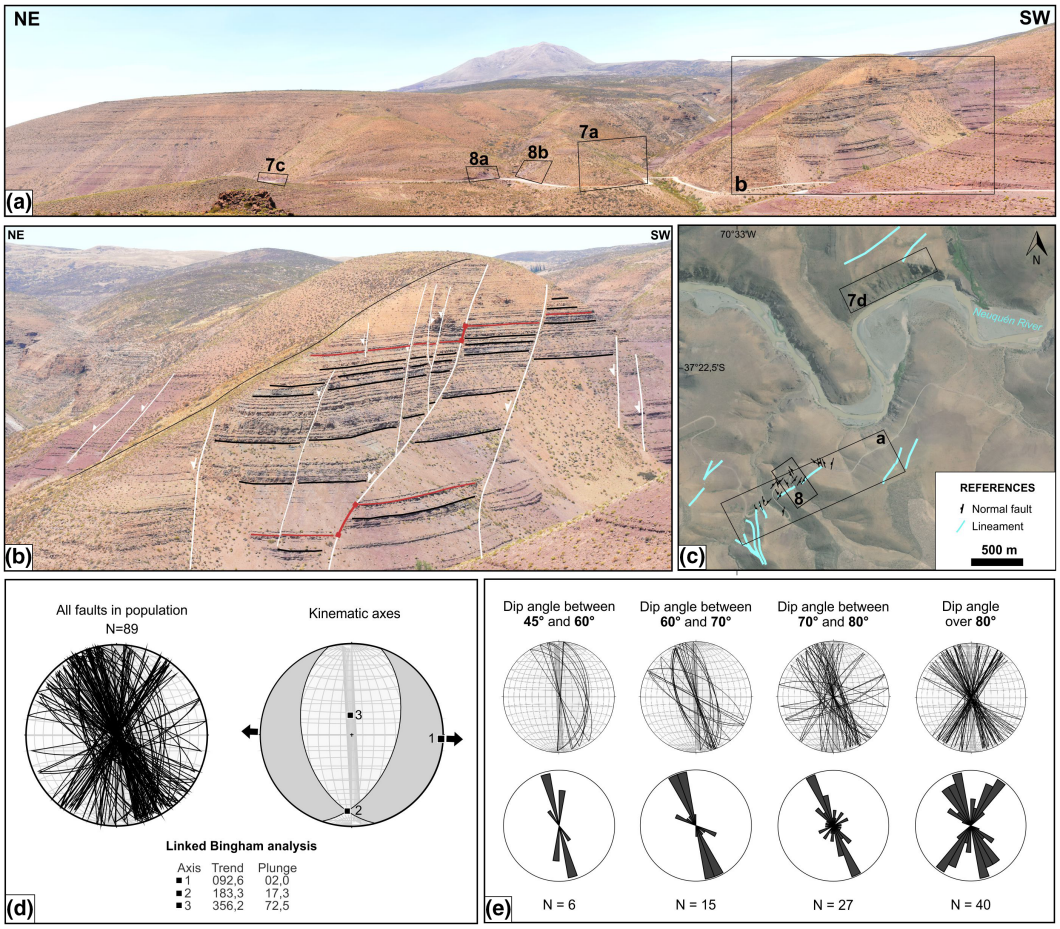

FIGURE 6 (a) Panoramic view of the Cordillera del Viento area showing extensional features in the Tordillo Formation (items 7a–7c in Figure 7, a and b in Figure 8 and b in this Figure). (b) Close-up view of extensional faults in the Tordillo Formation. Red lines show relative fault offset, which diminishes up-section. (c) Map view of normal fault traces (light blue lines) in the Cordillera del Viento area. Rectangles show the location of Figures 6a, 7e and 8. (d) Stereographic projections of fault planes from the complete dataset ($n = 89$) and the linked Bingham kinematic axes and fault plane solutions. Table shows kinematic axes orientation (1: extension; 2: intermediate; 3: shortening). Black arrows show the direction of extension. (e) Stereographic projections of fault planes and corresponding rose diagrams for the normal faults measured, as classified by dip values.

Damas Formation, along the western Chilean slope of the Andes (Figure 2b), and volcanic and plutonic rocks of a broader Jurassic age, in the Coastal Cordillera (Figure 1a). These results agree with previous provenance studies for adjoining areas (Naipauer, Tunik, et al., 2015; Spalletti et al., 2008). Paleocurrent data from our work and from previous works in the area show an eastward direction of transport, supporting the mentioned magmatic units as a source of sediment (Gulisano, 1988; Spalletti & Piñol, 2005).

Minor zircon age populations show that Lower-Middle Jurassic and Permian units provided subordinate source material to the Tordillo Formation. The Lower-Middle Jurassic Cuyo and Lotena Groups would have been exposed during the Late Jurassic along the Huincul Arch to the south (Figure 1) and formed an important source area for the southern part of the northwestern depocenter (Figure 11a; Gulisano, 1988; Naipauer et al., 2012, Naipauer, Tunik, et al., 2015; Spalletti & Piñol, 2005).

The Permian age peak can be attributed to the Choiyoi Group, whose input is generally considered evidence of an eastern source since it mainly crops out in the San Rafael and Las Matras eastern blocks (Figure 2) (Horton et al., 2016; Naipauer & Ramos, 2016). Although Permian ages are present in all Tordillo Formation samples, they appear as a minor source. Even in the eastern outcrops from La Yesera, the Permian age peak is not dominant, suggesting that the main sediment pathways were directed eastward from principal source areas in the west and southwest (Figure 11a).

5.2 | Palaeogeography of the Tordillo Formation

Previous research on the northwestern depocenter of the Neuquén Basin proposes that the Tordillo Formation recorded the transition from an alluvial fan to a playa lake

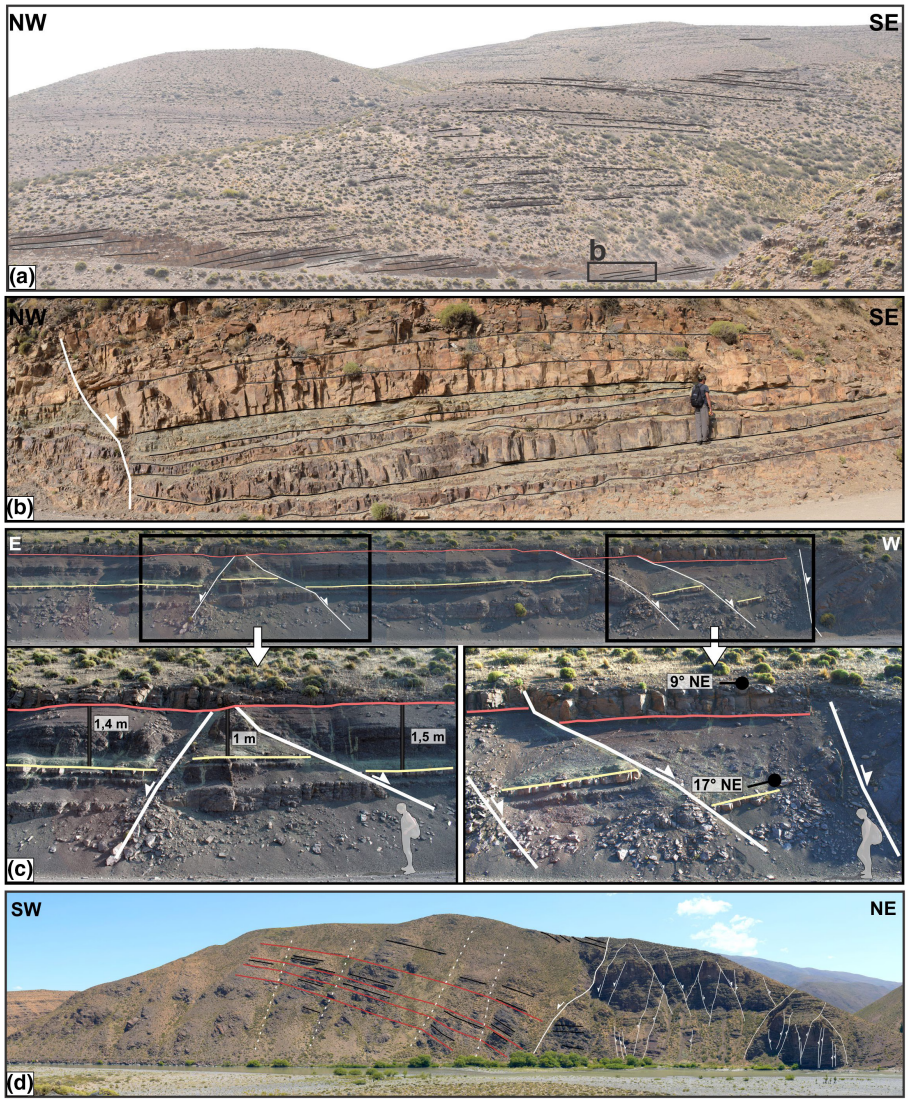

FIGURE 7 The Tordillo Formation in the Cordillera del Viento area. (a) Dip angle variations of the strata. The rectangle shows the location of b. (b) Wedge geometry of fine-grained strata and discontinuous sandstone beds, linked to a SE dipping normal fault. (c) E-W vertical section that exposes a series of normal faults that affect the thickness (left) and dip (right) of the beds. (d) Apparent rollover structure associated with an intensely fractured footwall on the northern side of the Neuquén River. White dotted lines indicate apparent axial planes (see Figure 6 for location).

depositional system (Coronel et al., 2020; Gulisano, 1988; Spalletti & Piñol, 2005; Spalletti & Veiga, 2007).

Based on our field observations at the Cerro Domuyo and Cordillera del Viento areas, we grouped the studied outcrops into two facies associations: channel deposits (FA1) and unconfined flow deposits (FA2). The first is present in the lower Cordillera del Viento section, the latter is dominant in the upper part of the Cordillera del Viento section and throughout the Domuyo section. The dominance of unconfined flows has been described in several depositional systems, such as the ephemeral fluvial, terminal flan/terminal splay and sheetflood-dominated alluvial fan (Blair, 1999, 2000; Fisher et al., 2008; Friend, 1977; Hampton & Horton, 2007; Kelly & Olsen, 1993; Sadler & Kelly, 1993; Turnbridge, 1981, 1984). This scenario is persistent in the central part of the basin, where a playa lake depositional system serves as inland drainage of the western clastic and volcaniclastic alluvial fans and, to a lesser extent, the southern and eastern fluvial systems (Figure 2b; Arregui, 1993; Spalletti et al., 2011; Spalletti & Veiga, 2007).

To understand the regional facies changes across the study area, we constructed stratigraphic transects based on the sections logged by Gulisano (1988) and Dellape (1976) (interpreted by Gulisano, 1988) (Figure 11b). Two main depositional environments were identified by Gulisano (1988): (i) the transition from alluvial fan to playa lake environments at the Loncopué,

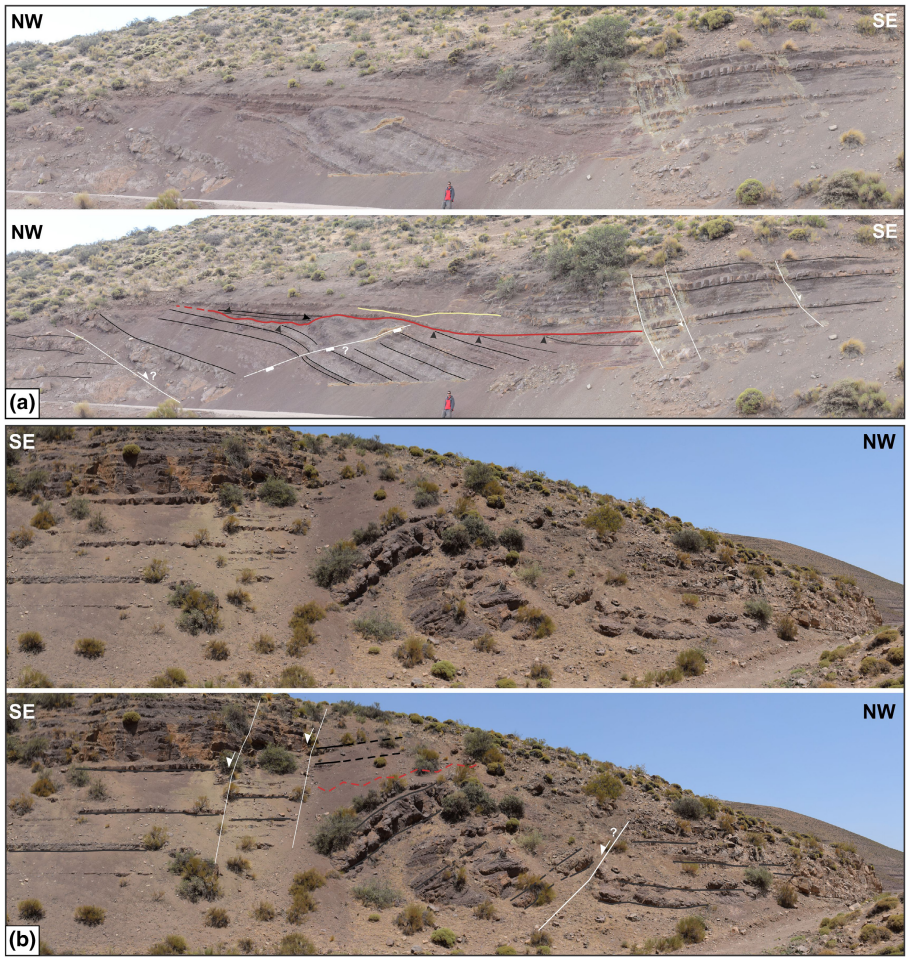

FIGURE 8 The Tordillo Formation in the Cordillera del Viento area. Opposite slopes of a creek show different vertical sections of the same structure. See Figure 6 for location. (a) Tilted strata, associated with normal faults and two angular unconformities (red and yellow lines). Black triangles show onlap and offlap relations. See the text for further description and interpretation. (b) Tilted strata with horizontal strata on top. The red dotted line indicates the position of the covered angular unconformity.

Cordillera del Viento and Cerro Domuyo areas (FA b1 to b5 from Gulisano, 1988), and (ii) lacustrine and sabkha environments at the La Yesera area to the east (FA c1 to c4 from Gulisano, 1988) (Figure 11b). These stratigraphical transects helped us to determine the vertical position of the Cordillera del Viento section within the Tordillo Formation column since neither the base nor the top of the unit crop out near the logged area (CV column in Figure 11b).

The greatest thickness values (ca. 700 m) for the Tordillo Formation in this region are at the Cordillera del Viento area (Figure 11b). In this area, the coarser grain facies (b1) also presents its maximum thickness and thins to the east (Gulisano, 1988). This pattern is consistent with our provenance results that indicate the main source of sediment was located to the west.

In the La Yesera area, the Tordillo Formation is ca. 100 m thick and records lacustrine deposition. Also, in this area, the top of the Auquilco evaporites presents sandstone-filled gullies that were eroded by karstic processes (Gulisano, 1988). Since palaeokarst features are indicators of subaerial exposure (Wright, 1988), the occurrence of karstic gullies at the La Yesera area suggests a period of non-deposition prior to lacustrine deposition.

Considering these characteristics, we interpret the alluvial filling of the western depocenter (between Loncopue and Cerro Domuyo) to have been contemporaneous with an eastern topographic high (La Yesera), but later became part of a fluvio-lacustrine system that drained the western and southern alluvial and fluvial systems (Figure 12a).

5.3 | Late Jurassic extensional stage

At the Cordillera del Viento and Cerro Domuyo areas, we found a series of normal faults affecting the Tordillo and lower Vaca Muerta formations. Some of these faults have elements that are characteristic of syndepositional

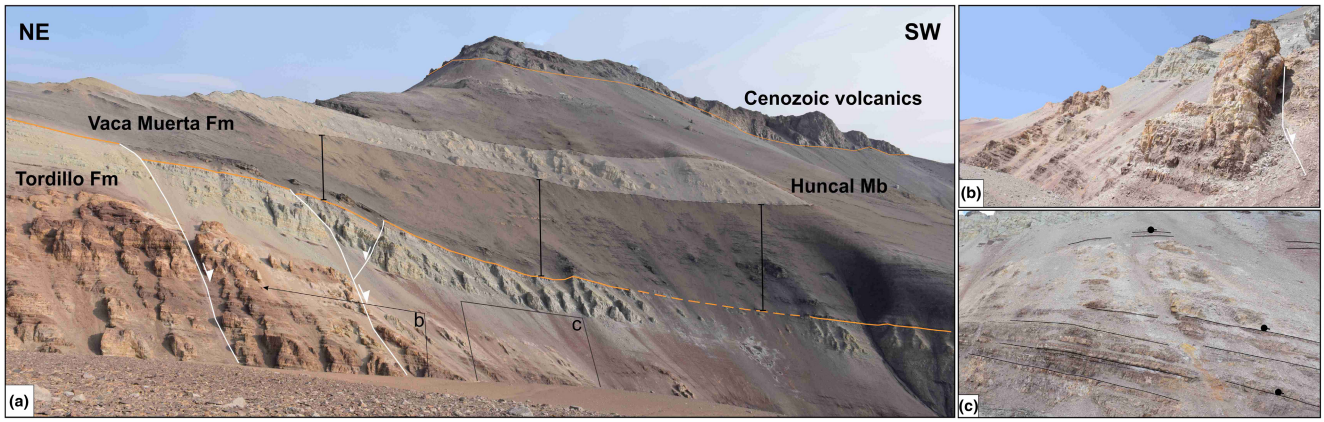

FIGURE 9 Photographs of the Tordillo and Vaca Muerta formations at the Covunco creek, Cerro Domuyo area. (a) Normal faults cutting the upper Tordillo Formation and lower Vaca Muerta Formation. The lower section of the Vaca Muerta Formation, between the Tordillo Formation and the Huncal Member, increases towards the SW (the Huncal Member is described by Kietzmann & Vennari, 2013). (b) Close-up view of a normal fault. (c) Dip variations in the upper Tordillo Formation.

extension, such as thickness variations of the strata between horst and grabens, dip angle variations, wedge geometry of the strata or are linked to angular unconformities (Figures 7b,c, 8 and 9) (Gibbs, 1983; Schlische, 1991; Scholz & Contreras, 1998). We observed normal faults with associated wedge-shaped strata, characterized by increasing both angle and thickness towards the fault plane (Figure 7b). In this outcrop, only the fine-grained strata show wedge-like geometries, while sandstone bodies appear discontinuous. This is consistent with models of alluvial deposition in half-grabens developed by Alexander and Leeder (1987). We recognized tilted strata overlaid by horizontal beds, which we interpret as angular unconformities. From the observation of the tilted strata from different vertical sections (Figure 8), we interpret that it could be associated with a NW dipping normal fault. Satellite images allowed us to identify a NE-trending lineament that cuts across the location of Figure 8 and coincides with the location of the inferred structure (Figure 6c).

We also observed a decrease in the offset of normal faults (Figure 6b), although this is not unequivocal of syndeposition, since it can be developed due to post-depositional deformation (Nicol et al., 1996; Walsh & Watterson, 1989). The complex structure shown in Figure 7d presents a similar arrangement as the analogue models for extensional basins developed by McClay (1990), however, it cannot be considered as evidence of syndeposition.

Evidence of extension during the Late Jurassic in the Neuquén Basin was previously described in the northern part of the basin (32°–35°S). In these sectors, the fundamental evidence in support of the extension is the volumetric magmatism of the Rio Damas Formation, emplaced in a retroarc position in reference to the Jurassic arc location (Figure 1a) (Charrier et al., 2007). Records of extensional faulting are scarce, restricted to isolated outcrops, inferred from balanced structural sections that require the addition of local graben and half-graben structures, or from isopach maps (Acevedo et al., 2020; Cegarra & Ramos, 1996; Giambiagi et al., 2003; Mardones et al., 2021; Martos et al., 2020; Mescua et al., 2008, 2014; Pángaro et al., 1996; Vicente & Leanza, 2009). These Late Jurassic normal faults have consistent NNW, N or NE strike directions, although some of them are inferred or indirectly measured (Figure 12c) (Acevedo et al., 2020; Cegarra & Ramos, 1996; Giambiagi et al., 2003; Mardones et al., 2021; Martos et al., 2022; Mescua et al., 2020; Pángaro et al., 1996).

In the southern portion of the basin (35°–41°S), there are fewer locations where the Late Jurassic has been associated with extensional activity (Figure 12c). At the Cerro Domuyo area, Galetto et al. (2021) interpret a north-trending normal fault that would have controlled the Tordillo Formation thickness, based on thermochronological data. In the Neuquén Embayment, Cristallini et al. (2006) recognize that some subsurface Late Triassic–Early Jurassic normal faults remained active during the Tordillo Formation deposition, although they attributed this to differential subsidence. Also, in the Neuquén Embayment, a series of *en-echelon* normal faults with a dominant NW trend affect the upper levels of the Tordillo Formation and lower levels of the Vaca Muerta Formation (Dominguez et al., 2017; Marchal et al., 2020).

In this scenario, the Late Jurassic extension has been mostly described in the northern part of the basin (32°–35°S) (Figure 12c). Considering the evidence we found for syndepositional extension within the Tordillo Formation and basal Vaca Muerta Formation, we propose that the Late Jurassic extension reached southern parts of the basin, at least as far as our study area, at ca. 37°S.

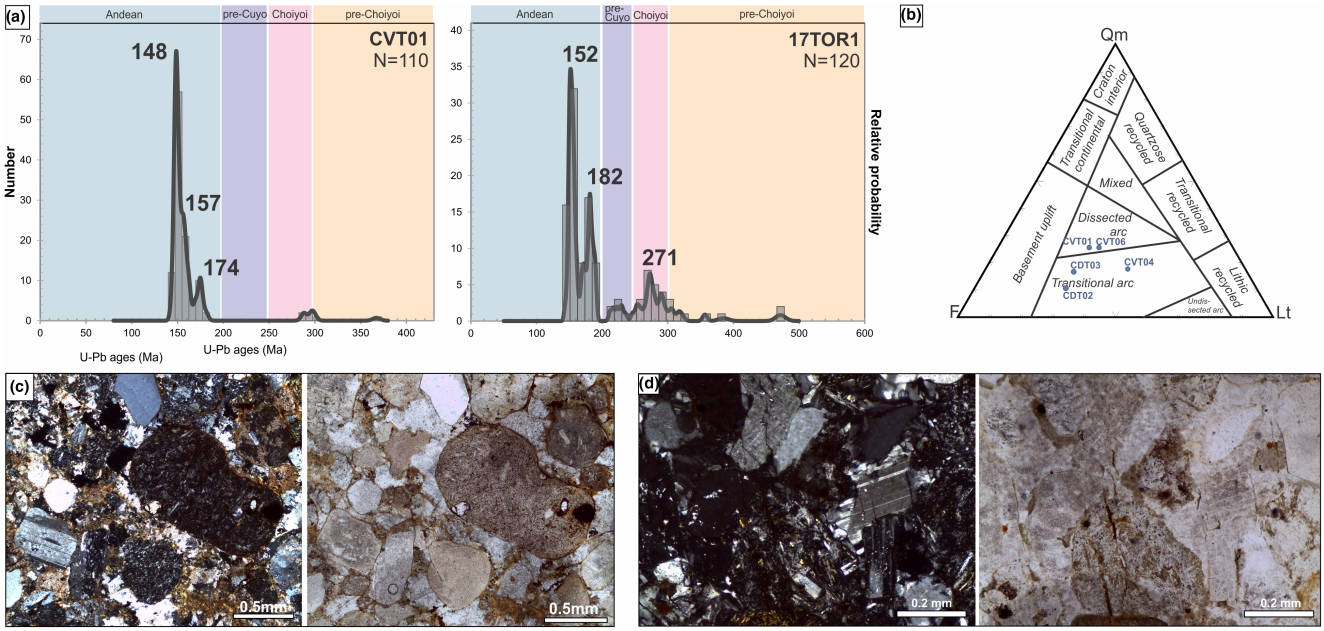

FIGURE 10 (a) Frequency histogram and relative probability plots of U–Pb ages of detrital zircons for CVT-01 and 17TOR1 samples of the Tordillo Formation from the Cordillera del Viento area. Time intervals of magmatism are from Sato et al. (2015). (b) Sandstone point count data plotted on Dickinson et al. (1983) provenance diagrams. (c) Photomicrographs of sample CVT-04. (d) Photomicrographs of sample CVT-01.

Mechanical rifting could be associated with dynamic uplift due to lithospheric thinning and low-density asthenosphere replacement (Ziegler & Cloetingh, 2004). In our proposed scenario, Late Jurassic regression would be forced due to rift dynamics.

5.4 | Late Triassic–Early Jurassic versus Late Jurassic extension

Our study sought to determine the structural framework of the study area (northwestern depocenter of the Neuquén Basin), compare it to other sectors of the basin and assess whether the Late Jurassic (Tordillo and lower Vaca Muerta formations) extensional stage reactivated the Late Triassic–Early Jurassic (Precuyo Group) fault systems of the initial opening of the Neuquén Basin. In Figure 12, we illustrate and compare the Late Triassic–Early Jurassic and Late Jurassic depocenters, fault trends and stress orientations.

In the Late Triassic–Early Jurassic depocenter in the Cordillera del Viento area (Chacay Melehue, Figure 12b) sedimentation would have been controlled by NW to WNW and NE striking normal faults (Sagripanti et al., 2014). Towards the east, the subsurface Early Jurassic Altiplanicie del Payún depocenter (Cara Cura-Reyes area, Figure 1b) is filled with up to 5 km of sediment and was controlled by WNW and ENE extensional faults (Figure 12b) (Fennell et al., 2020). The local minimum stress orientation for the adjacent Cara Cura-Reyes depocenter is NNE (Giambiagi et al., 2009), consistent with the NNE to NE regional extension direction calculated for the opening of the Neuquén Basin (Bechis et al., 2014).

When compared, stress orientation calculations show a significant difference: NNE to NE for the Late Triassic–Early Jurassic extension (Bechis et al., 2014) versus E-W for the Late Jurassic extension (this work) (Figure 12b,c). This is consistent with the lack of reactivation of initial rift structures during the Late Jurassic, which is particularly evident farther east in the Reyes-Cara Cura area where the Late Triassic–Early Jurassic Precuyo Group is 5 km thick, but the Tordillo Formation was not deposited or is <100 m thick (Fennell et al., 2020).

5.5 | Late Jurassic tectonic setting of the Neuquén Basin

Despite an extensional setting is proposed for the Tordillo Formation, compressional structures and an angular unconformity are recorded in the southern basin margin, at the Huincul Arch (Freije et al., 2002; Silvestro & Zubiri, 2008; Stipanicic & Rodrigo, 1970; Vergani et al., 1995; Zavala & Freije, 2002). The coexistence of extension in the north with uplift along the southern basin margin (Huincul Arch) has been previously discussed by Mescua et al. (2020), who suggested trench rollback and clockwise rotation of the South American

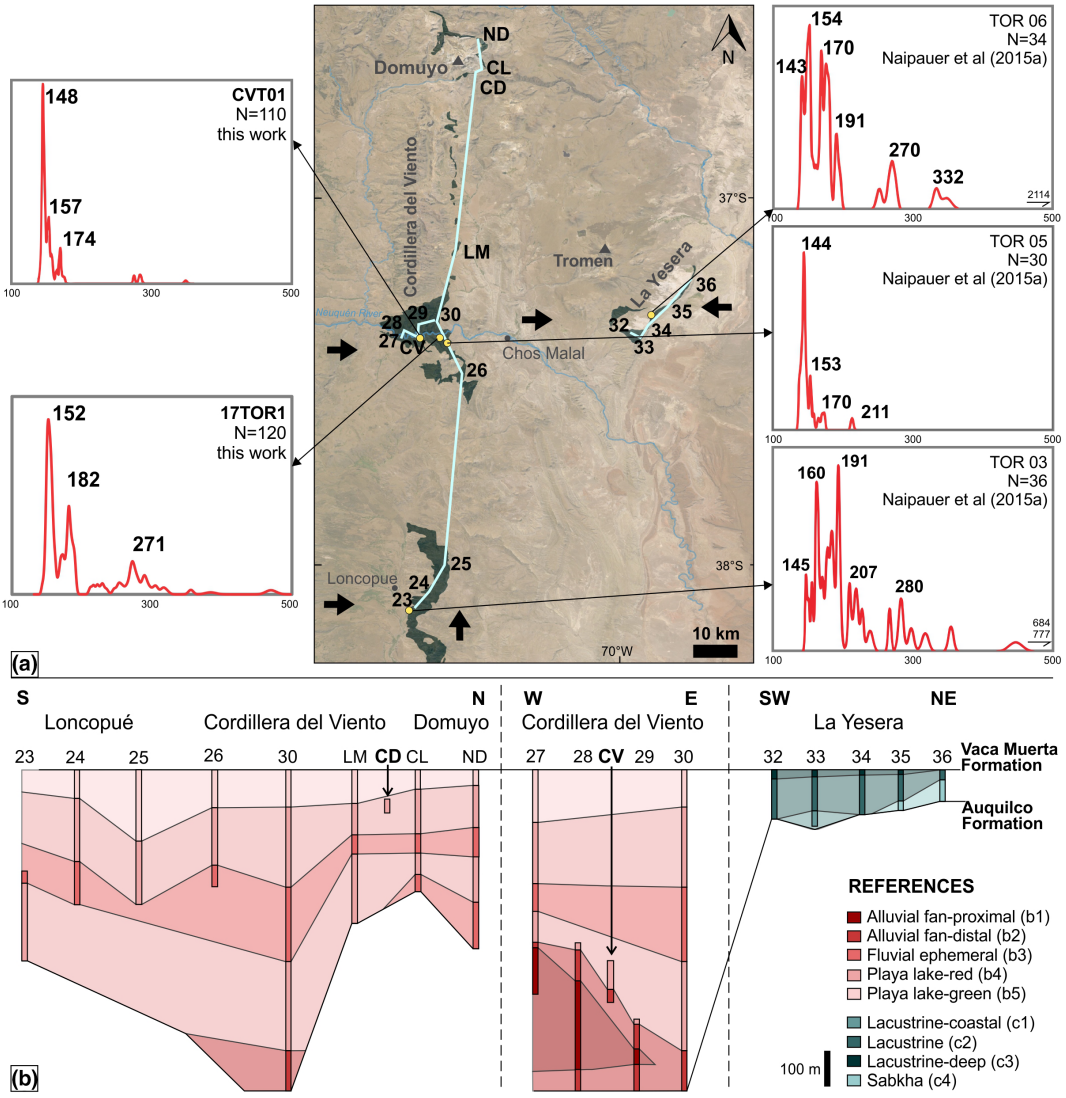

FIGURE 11 (a) U–Pb age distributions of the Tordillo Formation on the study area and its surroundings (samples from this work and Naipauer, Tunik, et al., 2015). Yellow dots mark sample locations; light blue lines on the map show the stratigraphic transects, black numbers and letters refer to the location of the stratigraphic sections shown in b in this Figure. Black arrows show the interpreted sediment route direction. (b) Stratigraphic transects showing lateral facies variations within the Tordillo Formation. Facies interpretations are from Gulisano (1988). Sedimentary sections are from this work (CD and CV), Gulisano (1988) (23 to 36) and Dellape (1976) interpreted by Gulisano (1988) (LM, CL and ND). Thickness values for incomplete sections are extrapolated from the isopach map of Gulisano (1988). The distance between sections is not to scale.

plate could explain this complex tectonic scenario. However, based on the presence of normal faults between the uppermost Tordillo Formation and the base of the Vaca Muerta Formation at the Huincul Arch area, Freije et al. (2002) propose that the latest Tordillo and the earliest Vaca Muerta formations were deposited in an extensional setting. These authors locate the compressional period in the lower terms of the Tordillo Formation deposition. Furthermore, Zavala et al. (2020) question the importance of the Late Jurassic uplift of the Huincul Arch, since they propose the major uplift of this area developed mainly during the Middle Jurassic. Thus, the Late Jurassic uplift at the Huincul Arch is still a matter of discussion.

In the Neuquén Embayment area, differential compaction of the Late Triassic Precuyo Group has been proposed as the subsidence mechanism controlling Tordillo Formation deposition (Cristallini et al., 2006). However, there are several key elements that discourage this interpretation in our study area and on a regional scale: (i) the extensional fault systems of the Precuyo Group and Tordillo Formation present significantly different orientations in the study area, while the example studied by Cristallini et al. (2006) only display fault reactivations; (ii) ca. 50 km to the east of the study area, at the Reyes-Cara Cura area, while near 5 km of Precuyo Group sediments were deposited, the Tordillo Formation is <100 m

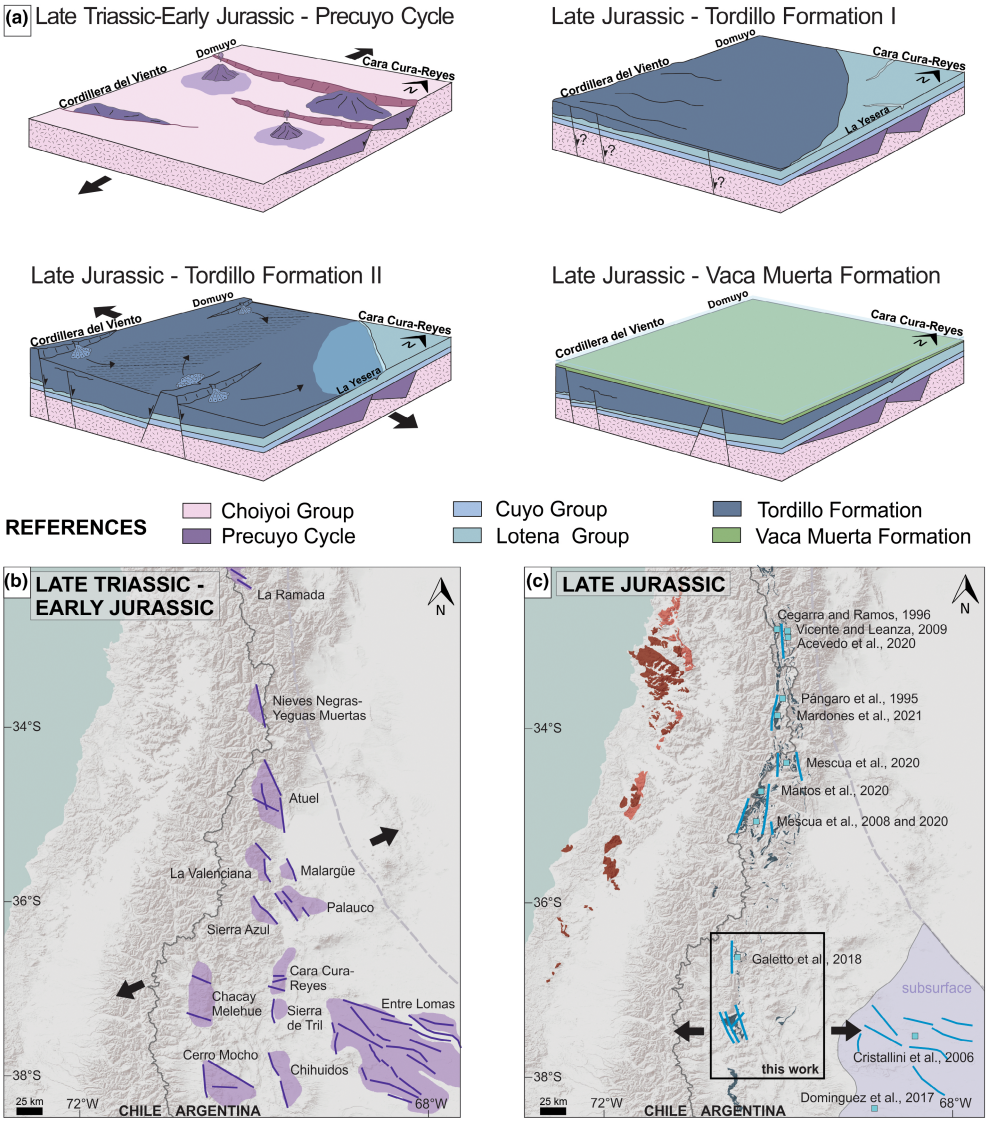

FIGURE 12 (a) Schematic paleogeographic evolution in the study area, comparing the Early Jurassic (based on Fennell et al., 2020) and the Late Jurassic extensional phases. The minimum stress orientation for the Precuyo is NNE and for the Tordillo is E-W. (b) Location of the Precuyo depocenters and its master faults (purple lines) throughout the Neuquén Basin. (c) Location of previous works that register the existence of extensional controls on the Tordillo Formation and their observed or inferred fault orientations (blue lines). The grey field indicates subsurface data.

thick or was not deposited (Fennell et al., 2020); (iii) in the northernmost Neuquén Basin (ca. 33°S), there is no record of Precuyo Group depocenters (Figure 12b), however, at these latitudes, there are several proposals of Late Jurassic extension (Acevedo et al., 2020; Cegarra & Ramos, 1996; Giambiagi et al., 2003; Vicente & Leanza, 2009); (iv) the Río Damas Formation (Chilean equivalent of the Tordillo Formation) reaches thickness values of 5 km (Klohn, 1960), which could not be explained only by differential compaction; (v) differential compaction associated faults would show maximum displacement in the lower post-rift and a gradual upwards decrease in throw, instead of discrete pulses of reactivation (Worthington & Walsh, 2017). On this basis, differential compaction cannot account for the magnitude of subsidence required to explain the Late Jurassic deposition of the Tordillo and Rio Damas Formations, though it might have been responsible to some degree as a secondary process.

Late Jurassic E-W extension appears restricted to the north-trending Andean axis (Figure 12c). In contrast, the Late Triassic–Early Jurassic rift, which marks the opening of the Neuquén Basin, involved extension that spanned the entire basin (including the Neuquén Embayment) (Figure 12b). Further, the Late Triassic–Early Jurassic extension reactivated previous lithospheric weaknesses that show a NNW to NW orientation (Figure 12b; Bechis et al., 2014). Late Jurassic extension

during Tordillo deposition did not reactivate these old structures, instead developed new ones with a NNW to N-S trend, parallel to the subduction zone and magmatic arc. The contrast between the architecture of these two extensional phases suggests different tectonic conditions during Late Triassic–Early Jurassic versus Late Jurassic extension.

The timespan of Tordillo sedimentation coincides with distributed intracontinental extension of Late Jurassic–Early Cretaceous age prior to the opening of the South Atlantic Ocean (Gust et al., 1985; Lovecchio et al., 2020; Uliana & Biddle, 1988); this extension orientation, as determined for the Colorado basin at 39°S, was WNW-ESE (Lovecchio et al., 2018). Also, rollback conditions have been proposed for the Late Jurassic at the latitude of the Neuquén Basin (Charrier et al., 2007; Mescua et al., 2020; Rossel et al., 2020). Therefore, the Late Jurassic stage of extension within the Neuquén Basin would be considered to be part of an extensional back-arc system boosted by rollback of the subducted slab and generalized extension prior to South Atlantic opening.

Traditional approaches analysing the Neuquén Basin had regarded it as a classic model of a rift basin governed by an initial mechanical rift and a posterior thermal subsidence phase (e.g. Legarreta & Gulisano, 1989). However, recent studies highlight subduction-related processes exerting a significant role in the evolution of the basin (Scivetti & Franzese, 2019; Tapia et al., 2020; Vicente, 2006). In this context, the Neuquén Basin does not behave as a simple rift system but has two synrift episodes that could be controlled by upper mantle dynamics related to changes in the subduction zone configuration.

6 | CONCLUSIONS

To elucidate the complex tectonic setting of the Late Jurassic Tordillo Formation in the Neuquén Basin, we studied outcrops at the Cerro Domuyo and southern Cordillera del Viento areas. We analysed the depositional environment, structure, provenance and then integrated the results into a palaeogeographical model for the Tordillo Formation sedimentation. We agree with previous studies in the area regarding the depositional environment, which is interpreted as part of a distal fan-playa lake depositional system. We recognized extensional structures active during the Tordillo sedimentation, with NNW to NW and NE fault orientations and an E-W-oriented minimum stress axis. These structures also affected the lower levels of the Vaca Muerta Formation at the Cerro Domuyo. Maximum depositional ages of 148.69 ± 0.27 and 151.88 ± 0.32 Ma for two samples of the Tordillo Formation are consistent with previous studies. Provenance analyses show that western magmatic zones formed the main sediment source for the Tordillo study area.

We add new evidence for Late Jurassic extension further south from previous works (ca. 37°S), which are localized at the northern portion of the basin (32°–35°S). When compared to the Late Triassic–Early Jurassic extension, a switch in stress orientation is observed, along with a lack of reactivation of pre-existing extensional faults. This contrast would indicate that the extensional mechanism had different origins. We consider Late Jurassic Tordillo extension to represent an extensional back-arc stage of the Neuquén Basin, induced by slab rollback and generalized extension during the initial stages of South Atlantic opening.

ACKNOWLEDGEMENTS

The authors thank Assistant Editor Craig Magee and reviewers, among them Nicolas Scivetti, for their insightful comments and suggestions, which have helped improve the manuscript. This work was supported by the Agencia Nacional de Promoción Científica y Tecnológica grant PICT- 2019-00974; CONICET grants PUE 22920160100051 and PIP 11220150100426CO; the Conicyt Fondecyt Regular project 1200428; the U.S. National Science Foundation grant EAR-1918541; and the University of Buenos Aires grant UBACyT 20020150100166BA. This is the R-440 contribution of the Instituto de Estudios Andinos Don Pablo Groeber (IDEAN, UBA-CONICET).

CONFLICT OF INTEREST

No, there is no conflict of interest.

PEER REVIEW

The peer review history for this article is available at https://publons.com/publon/10.1111/bre.12744.

DATA AVAILABILITY STATEMENT

The data that supports the findings of this study are available in the supplementary material of this article.

ORCID

Eliana Acevedo https://orcid.org/0000-0002-5377-1859
Lucía Fernández Paz https://orcid.org/0000-0001-5202-6809
Alfonso Encinas https://orcid.org/0000-0003-1519-1017
Brian K. Horton https://orcid.org/0000-0002-1402-3524
Victor Valencia https://orcid.org/0000-0003-2508-651X
Andrés Folguera https://orcid.org/0000-0001-8965-8543

REFERENCES

Acevedo, E., Rosselot, E. A., Martos, F., Fennell, L., Naipauer, M., & Folguera, A. (2020). Tectonic setting of the Tordillo formation

in the Aconcagua fold-and-thrust belt. In D. Kietzmann & A. Folguera (Eds.), *Opening and closure of the Neuquén Basin in the southern Andes* (pp. 159–174). Springer Earth System Sciences.

Alexander, J., & Leeder, M. R. (1987). Active tectonic control of alluvial architecture. In F. G. Ethridge, R. M. Flores, & M. D. Harvey (Eds.), *Recent developments in fluvial sedimentology* (pp. 243–252). SEPM, Special Publication 39.

Allen, J. R. (1977). The possible mechanics of convolute lamination in graded sand beds. *Journal of the Geological Society*, *134*(1), 19–31.

Allmendinger, R. W., Cardozo, N. C., & Fisher, D. (2012). *Structural geology algorithms: Vectors & tensors*. Cambridge University Press.

Arregui, C. (1993). Análisis estratigráfico paleoambiental de la Formación Tordillo en el subsuelo de la Cuenca Neuquina. *Actas XII Congreso Geológico Argentino y II Congreso de Exploración de Hidrocarburos*, *1*, 165–170.

Bechis, F., Cristallini, E. O., Giambiagi, L. B., Yagupsky, D. L., Guzmán, C. G., & García, V. H. (2014). Transtensional tectonics induced by oblique reactivation of previous lithospheric anisotropies during the late Triassic to early Jurassic rifting in the Neuquén basin: Insights from analog models. *Journal of Geodynamics*, *79*, 1–17.

Bechis, F., Giambiagi, L., García, V., Lanés, S., Cristallini, E., & Tunik, M. (2010). Kinematic analysis of a transtensional fault system: The Atuel depocenter of the Neuquén basin, southern Central Andes, Argentina. *Journal of Structural Geology*, *32*(7), 886–899.

Bechis, F., Giambiagi, L. B., Tunik, M. A., Suriano, J., Lanés, S., & Mescua, J. F. (2020). Tectono-stratigraphic evolution of the Atuel Depocenter during the late Triassic to early Jurassic rift stage, Neuquén Basin, west-Central Argentina. In D. Kietzmann & A. Folguera (Eds.), *Opening and closure of the Neuquén Basin in the southern Andes* (pp. 23–52). Springer Earth System Sciences.

Blair, T. C. (1999). Cause of dominance by sheetflood vs. debris-flow processes on two adjoining alluvial fans, Death Valley, California. *Sedimentology*, *46*(6), 1015–1028.

Blair, T. C. (2000). Sedimentology and progressive tectonic unconformities of the sheetflood-dominated Hell's gate alluvial fan, Death Valley, California. *Sedimentary Geology*, *132*(3–4), 233–262.

Borghi, P., Fennell, L., Omil, R. G., Naipauer, M., Acevedo, E., & Folguera, A. (2019). The Neuquén group: The reconstruction of a late cretaceous foreland basin in the southern Central Andes (35–37°S). *Tectonophysics*, *767*, 228177.

Bridge, J. S. (2003). *Rivers and floodplains: Forms, processes, and sedimentary record*. Blackwell.

Cegarra, M. I., & Ramos, V. A. (1996). La faja plegada y corrida del Aconcagua. In V. A. Ramos (Ed.), *Geología de la región del Aconcagua, provincias de San Juan y Mendoza* (pp. 387–422). Dirección Nacional del Servicio Geológico, Subsecretaría de Minería de la Nación.

Chang, Z., Vervoort, J. D., McClelland, W. C., & Knaack, C. (2006). U-Pb dating of zircon by LA-ICP-MS. *Geochemistry, Geophysics, Geosystems*, *7*(5), Q05009.

Charrier, R. (1981). Geologie der chilenischen Hauptkordillere zwischen 34° und 34°30′ südlicher Breite und ihre tektonische, magmatische und paläogeographische Entwicklung. *Berliner geowissenschaften Abhandlungen*, *A*(36), 270.

Charrier, R., Pinto, L., & Rodríguez, M. P. (2007). Tectonostratigraphic evolution of the Andean Orogen in Chile. In T. Moreno & W. Gibbons (Eds.), *The geology of Chile* (pp. 21–114). Geological Society of London.

Charrier, R., Ramos, V. A., Tapia, F., & Sagripanti, L. (2015). Tectono-stratigraphic evolution of the Andean Orogen between 31 and 37 S (Chile and Western Argentina). *Geological Society of London, Special Publications*, *399*(1), 13–61.

Collinson, J. D. (1996). Alluvial Sediments. In H. G. Reading (Ed.), *Sedimentary environments: Processes, facies and stratigraphy* (pp. 37–81). Blackwell Science.

Coronel, M. D., Isla, M. F., Veiga, G. D., Mountney, N. P., & Colombera, L. (2020). Anatomy and facies distribution of terminal lobes in ephemeral fluvial successions: Jurassic Tordillo formation, Neuquén Basin, Argentina. *Sedimentology*, *67*(5), 2596–2624.

Coutts, D. S., Matthews, W. A., & Hubbard, S. M. (2019). Assessment of widely used methods to derive depositional ages from detrital zircon populations. *Geoscience Frontiers*, *10*(4), 1421–1435.

Cristallini, E., Bottesi, G., Gavarrino, A., Rodríguez, L., Tomezzoli, R., & Comeron, R. (2006). Synrift geometry of the Neuquén Basin in northeastern Neuquén Province, Argentina. *Geological Society of America, Special Paper*, *407*, 147–161.

Davidson, J. (1988). El Jurásico y Cretácico inferior en las nacientes del río Teno (Chile): una revisión. *V Congreso Geológico Chileno*, *1*, 453–458.

D'Elia, L., Bilmes, A., Naipauer, M., Vergani, G. D., Muravchik, M., & Franzese, J. R. (2020). The Syn-rift of the Neuquén Basin (Precuyano and lower Cuyano cycle): Review of structure, volcanism, tectono-stratigraphy and depositional scenarios. In D. Kietzmann & A. Folguera (Eds.), *Opening and closure of the Neuquén Basin in the southern Andes* (pp. 3–21). Springer Earth System Sciences.

Dellape, D. A. (1976). *Informe mensual, Diciembre 1976. Comisión Geológica N° 1*. Yacimientos Petrolíferos Fiscales.

Di Giulio, A., Ronchi, A., Sanfilippo, A., Balgord, E. A., Carrapa, B., & Ramos, V. A. (2017). Cretaceous evolution of the Andean margin between 36 S and 40 S latitude through a multi-proxy provenance analysis of Neuquén Basin strata (Argentina). *Basin Research*, *29*(3), 284–304.

Dickinson, W. R., Beard, L. S., Brakenridge, G. R., Erjavec, J. L., Ferguson, R. C., Inman, K. F., Knepp, R. A., Lindberg, F. A., & Ryberg, P. T. (1983). Provenance of North American Phanerozoic sandstones in relation to tectonic setting. *Geological Society of America Bulletin*, *94*(2), 222–235.

Dickinson, W. R., & Gehrels, G. E. (2009). Use of U–Pb ages of detrital zircons to infer maximum depositional ages of strata: A test against a Colorado plateau Mesozoic database. *Earth and Planetary Science Letters*, *288*(1–2), 115–125.

Dominguez, R. F., Cristallini, E., & Leanza, H. A. (2017). *Evolución Tectono—Sedimentaria del Sistema Vaca Muerta—Quintuco (Tithoniano a Valanginiano Inferior) en el Engolfamiento Neuquino, Argentina* (pp. 31–37). Actas XX Congreso Geológico Argentino, S5.

Fennell, L. M., Folguera, A., Naipauer, M., Gianni, G., Rojas Vera, E. A., Bottesi, G., & Ramos, V. A. (2017). Cretaceous deformation of the southern Central Andes: Synorogenic growth strata in the Neuquén group (35° 30′–37°S). *Basin Research*, *29*, 51–72.

Fennell, L. M., Iannelli, S. B., Encinas, A., Naipauer, M., Valencia, V., & Folguera, A. (2019). Alternating contraction and extension

in the southern Central Andes (35°–37°S). *American Journal of Science*, *319*(5), 381–429.

Fennell, L. M., Naipauer, M., Borghi, P., Sagripanti, L., Pimentel, M., & Folguera, A. (2020). Early Jurassic intraplate extension in west-Central Argentina constrained by U-Pb SHRIMP dating: Implications for the opening of the Neuquén basin. *Gondwana Research*, *87*, 278–302.

Ferguson, R. I. (1977). Meander sinuosity and direction variance. *Geological Society of America Bulletin*, *88*(2), 212–214.

Fisher, J. A., Krapf, C. B., Lang, S. C., Nichols, G. J., & Payenberg, T. H. (2008). Sedimentology and architecture of the Douglas Creek terminal splay, Lake Eyre, Central Australia. *Sedimentology*, *55*(6), 1915–1930.

Fisher, J. A., Nichols, G. J., & Waltham, D. A. (2007). Unconfined flow deposits in distal sectors of fluvial distributary systems: Examples from the Miocene Luna and Huesca systems, northern Spain. *Sedimentary Geology*, *195*(1–2), 55–73.

Folk, R. L., Andrews, P. B., & Lewis, D. W. (1970). Detrital sedimentary rock classification and nomenclature for use in New Zealand. *New Zealand Journal of Geology and Geophysics*, *13*(4), 937–968.

Folguera, A., Ramos, V. A., Zapata, T., & Spagnuolo, M. G. (2007). Andean evolution at the Guañacos and Chos Malal fold and thrust belts (36 30′–37 S). *Journal of Geodynamics*, *44*(3–5), 129–148.

Franzese, J. R., & Spalletti, L. A. (2001). Late Triassic–early Jurassic continental extension in southwestern Gondwana: Tectonic segmentation and pre-break-up rifting. *Journal of South American Earth Sciences*, *14*(3), 257–270.

Freije, H., Azúa, G., González, R., Ponce, J. J., & Zavala, C. (2002). *Actividad tectónica sinsedimentaria en el Jurásico del sur de la Cuenca Neuquina* (p. 17). Actas V Congreso de Exploración y Desarrollo de Hidrocarburos.

Friend, P. F. (1977). Distinctive features of some ancient river systems. In A. D. Miall (Ed.), *Fluvial Sedimentology* (pp. 531–542). Canadian Society of Petroleum Geologists.

Galetto, A., Georgieva, V., García, V. H., Zattin, M., Sobel, E. R., Glodny, J., Bordese, S., Arzadún, G., Bechis, F., Caselli, A. T., & Becchio, R. (2021). Cretaceous and Eocene rapid cooling phases in the southern Andes (36°–37°S): Insights from low-temperature Thermochronology, U-Pb geochronology, and inverse thermal modeling from Domuyo area, Argentina. *Tectonics*, *40*(6), e2020TC006415.

Gallardo Jara, R. E., Ghiglione, M. C., & Rojas Galliani, L. (2019). Tectonic evolution of the southern austral-Magallanes Basin in Tierra del Fuego. *Latin American Journal of Sedimentology and Basin Analysis*, *26*(2), 127–154.

Gana, P., & Tosdal, R. (1996). Geocronología U-Pb y K-Ar en intrusivos del Paleozoico y Mesozoico de la Cordillera de la Costa, Región de Valparaíso, Chile. *Revista Geológica de Chile*, *23*(2), 151–164.

Gehrels, G., & Pecha, M. (2014). Detrital zircon U-Pb geochronology and Hf isotope geochemistry of Paleozoic and Triassic passive margin strata of western North America. *Geosphere*, *10*(1), 49–65.

Gehrels, G. E., Valencia, V. A., & Ruiz, J. (2008). Enhanced precision, accuracy, efficiency, and spatial resolution of U-Pb ages by laser ablation–multicollector–inductively coupled plasma–mass spectrometry. *Geochemistry, Geophysics, Geosystems*, *9*(3), Q03017.

Giacosa, R., Allard, J., Foix, N., & Heredia, N. (2014). Stratigraphy, structure and geodynamic evolution of the Paleozoic rocks in the cordillera del Viento (37°S latitude, Andes of Neuquén, Argentina). *Journal of Iberian Geology*, *40*(2), 331–348.

Giambiagi, L., Tunik, M., Barredo, S., Bechis, F., Ghiglione, M., Alvarez, P., & Drosina, M. (2009). Cinemática de apertura del sector norte de la cuenca Neuquina. *Revista de la Asociación Geológica Argentina*, *65*(2), 278–292.

Giambiagi, L. B., Alvarez, P. P., Godoy, E., & Ramos, V. A. (2003). The control of pre-existing extensional structures on the evolution of the southern sector of the Aconcagua fold and thrust belt, southern Andes. *Tectonophysics*, *369*(1–2), 1–19.

Gibbs, A. D. (1983). Balanced cross-section construction from seismic sections in areas of extensional tectonics. *Journal of Structural Geology*, *5*(2), 153–160.

Gradstein, F. M., Ogg, J. G., Schmitz, M. D., & Ogg, G. M. (2020). *The geologic time scale 2020*. Elsevier.

Grier, M. E., Salfity, J. A., & Allmendinger, R. W. (1991). Andean reactivation of the cretaceous Salta rift, northwestern Argentina. *Journal of South American Earth Sciences*, *4*(4), 351–372.

Groeber, P. (1933). *Hoja 31c, Confluencia de los Ríos Grande y Barrancas*. Dirección General de Minas, Geología e Hidrología.

Groeber, P., Stipanicic, P. N., & Mingramm, A. (1953). Jurásico. In *Geografía de la República Argentina* (Vol. *2*, pp. 143–347). Sociedad Argentina Estudios Geográficos GAEA.

Guillaume, B., Martinod, J., & Espurt, N. (2009). Variations of slab dip and overriding plate tectonics during subduction: Insights from analogue modelling. *Tectonophysics*, *463*(1–4), 167–174.

Gulisano, C. A. (1988). *Análisis estratigráfico y sedimentológico de la Formación Tordillo en el oeste de la Provincia del Neuquén, Cuenca Neuquina, Argentina* [Unpublished doctoral dissertation]. Universidad de Buenos Aires.

Gulisano, C. A. (1993). Ciclo Precuyano. In A. C. Riccardi & S. E. Damborenea (Eds.), *Léxico estratigráfico de la Argentina. Volumen 9: Jurásico* (Vol. *21*, pp. 334–335). Asociación Geológica Argentina, B.

Gust, D. A., Biddle, K. T., Phelps, D. W., & Uliana, M. A. (1985). Associated middle to late Jurassic volcanism and extension in southern South America. *Tectonophysics*, *116*(3–4), 223–253.

Guzmán, C., Tapia, F., Ambrosio, A., Pleimling, A. G., Bustos, G., Gómez, C., & González, J. M. (2021). Lower Jurassic deformation in the eastern Huincul high, Argentina. *Journal of South American Earth Sciences*, *109*, 103295.

Hampton, B. A., & Horton, B. K. (2007). Sheetflow fluvial processes in a rapidly subsiding basin, Altiplano plateau, Bolivia. *Sedimentology*, *54*, 1121–1147.

Haq, B. U. (2018). Jurassic sea-level variations: A reappraisal. *GSA Today*, *28*(1), 4–10.

Heredia, N., García-Sansegundo, J., Gallastegui, G., Farias, P., Giacosa, R. E., Giambiagi, L. B., Busquets, P., Colombo, F., Charrier, R., Cuesta, A., Rubio-Ordóñez, A., & Ramos, V. A. (2018). Review of the geodynamic evolution of the SW margin of Gondwana preserved in the Central Andes of Argentina and Chile (28°-38° S latitude). *Journal of South American Earth Sciences*, *87*, 87–94.

Horn, B. L. D., Goldberg, K., & Schultz, C. L. (2018). Interpretation of massive sandstones in ephemeral fluvial settings: A case study from the upper Candelária sequence (upper Triassic, Paraná Basin, Brazil). *Journal of South American Earth Sciences*, *81*, 108–121.

Horton, B. K. (2018). Tectonic regimes of the central and southern Andes: Responses to variations in plate coupling during subduction. *Tectonics*, *37*(2), 402–429.

Horton, B. K., & Fuentes, F. (2016). Sedimentary record of plate coupling and decoupling during growth of the Andes. *Geology*, *44*(8), 647–650.

Horton, B. K., Fuentes, F., Boll, A., Starck, D., Ramirez, S. G., & Stockli, D. F. (2016). Andean stratigraphic record of the transition from backarc extension to orogenic shortening: A case study from the northern Neuquén Basin, Argentina. *Journal of South American Earth Sciences*, *71*, 17–40.

Howell, J. A., Schwarz, E., Spalletti, L. A., & Veiga, G. D. (2005). The Neuquén basin: An overview. *Geological Society of London, Special Publications*, *252*(1), 1–14.

Ingersoll, R. V., Bullard, T. F., Ford, R. L., Grimm, J. P., Pickle, J. D., & Sares, S. W. (1984). The effect of grain size on detrital modes: A test of the Gazzi-Dickinson point-counting method. *Journal of Sedimentary Research*, *54*(1), 103–116.

Jarrard, R. D. (1986). Relations among subduction parameters. *Reviews of Geophysics*, *24*(2), 217–284.

Junkin, W. D., & Gans, P. B. (2019). Stratigraphy and geochronology of the Nacientes del Teno and Río Damas formations: Insights into middle to late Jurassic Andean volcanism. *Geosphere*, *15*(2), 450–479.

Kelly, S. B., & Olsen, H. (1993). Terminal fans—A review with reference to Devonian examples. *Sedimentary Geology*, *85*, 339–374.

Kietzmann, D. A., Llanos, M. P. I., & Martínez, M. K. (2018). Astronomical Calibration of the Tithonian–Berriasian in the Neuquén Basin, Argentina: A Contribution from the Southern Hemisphere to the Geologic Time Scale. In M. Montenari (Ed.), *Stratigraphy & timescales* (Vol. *3*, pp. 327–355). Academic Press.

Kietzmann, D. A., Palma, R. M., & Llanos, M. P. I. (2015). Cyclostratigraphy of an orbitally-driven Tithonian–Valanginian carbonate ramp succession, southern Mendoza, Argentina: Implications for the Jurassic–cretaceous boundary in the Neuquén Basin. *Sedimentary Geology*, *315*, 29–46.

Kietzmann, D. A., & Vennari, V. V. (2013). Sedimentología y estratigrafía de la Formación Vaca Muerta (Tithoniano-Berriasiano) en el área del cerro Domuyo, norte de Neuquén, Argentina. *Andean Geology*, *40*(1), 41–65.

Kleiman, L. E., & Japas, M. S. (2009). The Choiyoi volcanic province at 34 S–36 S (San Rafael, Mendoza, Argentina): Implications for the late Palaeozoic evolution of the southwestern margin of Gondwana. *Tectonophysics*, *473*(3–4), 283–299.

Klohn, C. (1960). Geología de la Cordillera de los Andes de Chile Central, provincia de Santiago, O'Higgins, Colchagua y Curicoó. *Instituto Investigaciones Geológicas Boletín*, *8*, 1–95.

Lallemand, S., Heuret, A., & Boutelier, D. (2005). On the relationships between slab dip, back-arc stress, upper plate absolute motion, and crustal nature in subduction zones. *Geochemistry, Geophysics, Geosystems*, *6*(9), Q09006.

Leanza, H. A. (2003). Las sedimentitas huitrinianas y rayosianas (Cretácico Inferior) en el ámbito central y meridional de la Cuenca Neuquina, Argentina. *Servicio Geológico Minero Argentino, Serie Contribuciones Técnicas-Geología*, *2*, 1–31.

Leanza, H. A. (2009). Las principales discordancias del Mesozoico de la Cuenca Neuquina según observaciones de superficie. *Revista del Museo Argentino de Ciencias Naturales*, *11*(2), 145–184.

Leanza, H. A., Hugo, C. A., Repol, D., González, R., Danieli, J. C., & Lizuaín, A. (2001). *Hoja Geológica 3969-I Zapala*. Servicio Geológico Minero Argentino. Instituto de Geología y Recursos Minerales.

Leanza, H. A., Llambías, E. J., & Carbone, O. (2005). *Unidades estratigráficas limitadas por discordancias en los depocentros de la cordillera del Viento y la sierra de Chacaico durante los inicios de la cuenca Neuquina* (p. 13). Actas VI Congreso de exploración de hidrocarburos.

Leeder, M. R. (1999). *Sedimentology and sedimentary basins*. Blackwell.

Legarreta, L., & Gulisano, C. A. (1989). Análisis estratigráfico secuencial de la Cuenca Neuquina (Triásico Superior-Terciario Inferior). In G. Chebli & L. Spalletti (Eds.), *Cuencas Sedimentarias Argentinas* (Vol. *6*, pp. 221–243). Serie Correlación Geológica.

Legarreta, L., & Uliana, M. A. (1991). Jurassic-cretaceous marine oscillations and geometry of back-arc basin fill, central argentine Andes. In D. I. M. McDonald (Ed.), *Sedimentation, tectonics and Eustasy Sea-level changes at active margins* (Vol. *12*, pp. 429–450). International Association of Sedimentologists, Special Publication.

Legarreta, L., & Uliana, M. A. (1996). The Jurassic succession in west-Central Argentina: Stratal patterns, sequences and paleogeographic evolution. *Palaeogeography, Palaeoclimatology, Palaeoecology*, *120*(3–4), 303–330.

Lena, L., López-Martínez, R., Lescano, M., Aguire-Urreta, B., Concheyro, A., Vennari, V., Naipauer, M., Samankassou, E., Pimentel, M., Ramos, V. A., & Schaltegger, U. (2019). High-precision U–Pb ages in the early Tithonian to early Berriasian and implications for the numerical age of the Jurassic–cretaceous boundary. *Solid Earth*, *10*(1), 1–14.

Llambías, E. J., Leanza, H. A., & Carbone, O. (2007). Evolución tectono-magmática durante el Pérmico al Jurásico Temprano en la cordillera del Viento (37 05 S–37 15 S): nuevas evidencias geológicas y geoquímicas del inicio de la cuenca Neuquina. *Revista de la Asociación Geológica Argentina*, *62*(2), 217–235.

Llambıas, E. J., Quenardelle, S., & Montenegro, T. (2003). The Choiyoi group from Central Argentina: A subalkaline transitional to alkaline association in the craton adjacent to the active margin of the Gondwana continent. *Journal of South American Earth Sciences*, *16*(4), 243–257.

Lo Forte, G. L. (1996). Los depósitos jurásicos de la Alta Cordillera de Mendoza. In V. A. Ramos (Ed.), *Geología de la región del Aconcagua, provincias de San Juan y Mendoza* (pp. 179–230). Dirección Nacional del Servicio Geológico, Subsecretaría de Minería de la Nación.

Lovecchio, J. P., Rohais, S., Joseph, P., Bolatti, N. D., Kress, P. R., Gerster, R., & Ramos, V. A. (2018). Multistage rifting evolution of the Colorado basin (offshore Argentina): Evidence for extensional settings prior to the South Atlantic opening. *Terra Nova*, *30*(5), 359–368.

Lovecchio, J. P., Rohais, S., Joseph, P., Bolatti, N. D., & Ramos, V. A. (2020). Mesozoic rifting evolution of SW Gondwana: A polyphased, subduction-related, extensional history responsible for basin formation along the Argentinean Atlantic margin. *Earth-Science Reviews*, *203*, 103138.

Ludwig, K. R. (2003). Isoplot 3.00: A geochronological toolkit for Microsoft excel. *Berkeley Geochronology Center Special Publication*, *4*, 70.

Marchal, D., Manceda, R., Domínguez, R. F., & Sattler, F. (2020). Structural geology: Tectonic history, macrostructures, regional

fault map, fault systems, second-order structures, and impact of the inheritance. In D. Minisini, M. Fantín, M. Lanusse Noguera, & H. A. Leanza (Eds.), *Integrated geology of unconventionals: The case of the Vaca Muerta play, Argentina* (Vol. *121*, pp. 99–140). American Association of Petroleum Geologists Memoir.

Mardones, V., Peña, M., Pairoa, S., Ammirati, J. B., & Leisen, M. (2021). Architecture, kinematics, and tectonic evolution of the principal cordillera of the Andes in Central Chile (ca. 33.5°S): Insights from detrital zircon U-Pb geochronology and Seismotectonics implications. *Tectonics*, *40*(7), e2020TC006499.

Maretto, H., & Pangaro, F. (2005). *Edad de formación de algunas de las grandes estructuras del engolfamiento de la Cuenca Neuquina: actividad tectónica durante la depositación de la Fm*. Actas VI Congreso de exploración y Desarrollo de Hidrocarburos.

Marrett, R. A., & Allmendinger, R. W. (1990). Kinematic analysis of fault-slip data. *Journal of Structural Geology*, *12*, 973–986.

Martos, F. E., Fennell, L. M., Brisson, S., Palmieri, G., Naipauer, M., & Folguera, A. (2020). Tectonic evolution of the northern Malargüe fold and Thrust Belt, Mendoza province, Argentina. *Journal of South American Earth Sciences*, *103*, 102711.

Martos, F. E., Fennell, L. M., Naipauer, M., & Folguera, A. (2022). *Evolución tectónica del segmento norte de la faja plegada y corrida de Malargüe (34° 30'S)* (pp. 1227–1228). Actas XXI Congreso Geológico Argentino.

McClay, K. R. (1990). Extensional fault systems in sedimentary basins: A review of analogue model studies. *Marine and Petroleum Geology*, *7*(3), 206–233.

Mescua, J. F., Giambiagi, L. B., & Bechis, F. (2008). Evidencias de tectónica extensional en el Jurásico tardío (Kimeridgiano) del suroeste de la provincia de Mendoza. *Revista de la Asociación Geológica Argentina*, *63*(4), 512–519.

Mescua, J. F., Giambiagi, L. B., Tassara, A., Gimenez, M., & Ramos, V. A. (2014). Influence of pre-Andean history over Cenozoic foreland deformation: Structural styles in the Malargüe fold-and-thrust belt at 35 S, Andes of Argentina. *Geosphere*, *10*(3), 585–609.

Mescua, J. F., Suriano, J., Schencman, L. J., Giambiagi, L. B., Sruoga, P., Balgord, E., & Bechis, F. (2020). Controls on deposition of the Tordillo formation in southern Mendoza (34°–36°S): Implications for the Kimmeridgian tectonic setting of the Neuquén Basin. In D. Kietzmann & A. Folguera (Eds.), *Opening and closure of the Neuquén Basin in the southern Andes* (pp. 127–157). Springer Earth System Sciences.

Miall, A. D. (1977). A review of the braided-river depositional environment. *Earth-Science Reviews*, *13*(1), 1–62.

Miall, A. D. (1996). *The geology of fluvial deposits: Sedimentary Facies, basin analysis and petroleum geology*. Springer-Verlag.

Micucci, E., Bande, A., Starck, D., & Veiga, R. (2018). *El jurásico del Dorso de los Chihuidos, contribución a su conocimiento* (pp. 437–460). Actas X Congreso de Exploración y Desarrollo de Hidrocarburos.

Mosquera, A., & Ramos, V. A. (2006). Intraplate deformation in the Neuquén embayment. In S. M. Kay & V. A. Ramos (Eds.), *Evolution of an Andean margin: A tectonic and magmatic view from the Andes to the Neuquén Basin (35°–39°S lat)* (Vol. *407*, pp. 97–124). Geological Society of America, Special Paper.

Mpodozis, C., & Ramos, V. A. (1989). The Andes of Chile and Argentina. In G. E. Ericksen, M. T. Cañas Pinochet, & J. A. Reinemund (Eds.), *Geology of the Andes and its relation to hydrocarbon and mineral resources* (Vol. *11*, pp. 59–90). Circum-Pacific Council for Energy and Mineral Resources Earth Science Series.

Naipauer, M., Morabito, E. G., Marques, J. C., Tunik, M., Vera, E. A. R., Vujovich, G. I., Pimentel, M., & Ramos, V. A. (2012). Intraplate late Jurassic deformation and exhumation in western Central Argentina: Constraints from surface data and U–Pb detrital zircon ages. *Tectonophysics*, *524*, 59–75.

Naipauer, M., & Ramos, V. A. (2016). Changes in source areas at Neuquén Basin: Mesozoic evolution and tectonic setting based on U–Pb ages on zircons. In A. Folguera, M. Naipauer, L. Sagripanti, M. Ghiglione, D. Orts, & L. Giambiagi (Eds.), *Growth of the southern Andes* (pp. 33–61). Springer Earth System Sciences.

Naipauer, M., Tapia, F., Mescua, J. F., Farías, M., Pimentel, M., & Ramos, V. A. (2015). Detrital and volcanic zircon U-Pb ages from southern Mendoza (Argentina): An insight on the source regions in the northern part of Neuquén Basin. *Journal of South American Earth Sciences*, *64*(2), 434–451.

Naipauer, M., Tunik, M., Marques, J. C., Rojas Vera, E., Vujovich, G., Pimentel, M., & Ramos, V. A. (2015). U–Pb detrital zircon ages of upper Jurassic continental successions: Implications for the provenance and absolute age of the Jurassic–cretaceous boundary in the Neuquén Basin. In S. A. Sepúlveda, L. B. Giambiagi, S. M. Moreiras, L. Pinto, M. Tunik, G. D. Hoke, & M. Farías (Eds.), *Geodynamic processes in the Andes of Central Chile and Argentina* (Vol. *399*, pp. 131–154). Geological Society of London, Special Publications.

Narciso, V., Santamaría, G., & Zanettini, J. C. M. (2004). *Hoja Geológica 3769-I, Barrancas. Provincias de Mendoza y Neuquén*. Instituto de Geología y Recursos Minerales, Servicio Geológico Minero Argentino.

Nicol, A., Watterson, J., Walsh, J. J., & Childs, C. (1996). The shapes, major axis orientations and displacement patterns of fault surfaces. *Journal of Structural Geology*, *18*(2–3), 235–248.

Owen, G., Moretti, M., & Alfaro, P. (2011). Recognizing triggers for soft-sediment deformation: Current understanding and future directions. *Sedimentary Geology*, *235*(3–4), 133–140.

Pángaro, F., Ramos, V. A., & Godoy, E. (1996). La faja plegada y corrida de la Cordillera Principal de Argentina y Chile a la latitud del Cerro Palomares (33 35'S). *Actas XIII Congreso Geológico Argentino y III Congreso de Exploración de Hidrocarburos*, *2*, 315–324.

Parra, M., Mora, A., Jaramillo, C., Strecker, M. R., Sobel, E. R., Quiroz, L., Rueda, M., & Torres, V. (2009). Orogenic wedge advance in the northern Andes: Evidence from the Oligocene-Miocene sedimentary record of the Medina Basin, eastern cordillera, Colombia. *Geological Society of America Bulletin*, *121*(5–6), 780–800.

Ploszkiewicz, J. V., Orchuela, I. A., Vaillard, J., & Viñes, R. F. (1984). Compresión y desplazamiento lateral en la zona de falla Huincul, estructuras asociadas, Provincia del Neuquén. *Actas IX Congreso Geológico Argentino*, *2*, 163–169.

Ramos, V. A. (1977). Estructura de la Provincia de Neuquén. In E. O. Rolleri (Ed.), *Geología y Recursos Naturales de la Provincia del Neuquén. Relatorio del VII Congreso Geológico Argentino* (pp. 9–24). Asociación Geológica Argentina.

Ramos, V. A. (1981). *Descripción geológica de la Hoja 33c, Los Chihuidos Norte*. Servicio Geológico Nacional.

Ramos, V. A. (1985). El Mesozoico de la Alta Cordillera de Mendoza: Reconstrucción tectónica de sus facies. *Actas IV Congreso Geológico Chileno*, *1*, 104–118.

Ramos, V. A. (2010). The tectonic regime along the Andes: Present-day and Mesozoic regimes. *Geological Journal*, *45*(1), 2–25.

Ramos, V. A., & Folguera, A. (2005). Tectonic evolution of the Andes of Neuquén: Constraints derived from the magmatic arc and foreland deformation. *Geological Society, London, Special Publications*, *252*(1), 15–35.

Ramos, V. A., Jordan, T. E., Allmendinger, R. W., Mpodozis, C., Kay, S. M., Cortés, J. M., & Palma, M. (1986). Paleozoic terranes of the central Argentine-Chilean Andes. *Tectonics*, *5*(6), 855–880.

Rojas Vera, E. R., Mescua, J., Folguera, A., Becker, T. P., Sagripanti, L., Fennell, L., Orts, D., & Ramos, V. A. (2015). Evolution of the Chos Malal and Agrio fold and thrust belts, Andes of Neuquén: Insights from structural analysis and apatite fission track dating. *Journal of South American Earth Sciences*, *64*, 418–433.

Rossel, P., Echaurren, A., Ducea, M. N., Maldonado, P., & Llanos, K. (2020). Jurassic segmentation of the early Andean magmatic province in southern Central Chile (35–39°S): Petrological constrains and tectonic drivers. *Lithos*, *364*, 105510.

Rossel, P., Oliveros, V., Mescua, J. F., Tapia, F., Ducea, M. N., Calderón, S., Charrier, R., & Hoffman, D. (2014). The upper Jurassic volcanism of the Río Damas-Tordillo formation (33°–35.5°S): Insights on petrogenesis, chronology, provenance and tectonic implications. *Andean Geology*, *41*(3), 529–557.

Rovere, E. I., Caselli, A., Tourun, S., Leanza, H. A., Hugo, C. A., Folguera, A., Escosteguy, L., Geuna, S., González, R., Colombino, J., & Danieli, J. C. (2004). *Hoja Geológica 3772-IV, Andacollo, provincia del Neuqúen*. Instituto de Geología y Recursos Minerales. Servicio Geológico Minero Argentino.

Russo, R. M., & Silver, P. G. (1996). Cordillera formation, mantle dynamics, and the Wilson cycle. *Geology*, *24*(6), 511–514.

Sadler, S. P., & Kelly, S. B. (1993). Fluvial processes and cyclicity in terminal fan deposits: An example from the late Devonian of Southwest Ireland. *Sedimentary Geology*, *85*, 375–386.

Sagripanti, L., Folguera, A., Giménez, M., Vera, E. R., Fabiano, J. J., Molnar, N., Fennell, L., & Ramos, V. A. (2014). Geometry of middle to late Triassic extensional deformation pattern in the cordillera del Viento (southern Central Andes): A combined field and geophysical study. *Journal of Iberian Geology*, *40*(2), 349–366.

Sánchez, N., Turienzo, M., Lebinson, F., Araujo, V., Coutand, I., & Dimieri, L. (2015). Structural style of the Chos Malal fold and thrust belt, Neuquén basin, Argentina: Relationship between thick-and thin-skinned tectonics. *Journal of South American Earth Sciences*, *64*, 399–417.

Sanguinetti, A. S. (1989). Volcanismo neojurásico-neocomiano de la Quebrada de Vargas, Alta Cordillera de Mendoza. *Revista de la Asociación Geológica Argentina*, *44*(1–4), 381–393.

Sato, A. M., Llambías, E. J., Basei, M. A., & Castro, C. E. (2015). Three stages in the late Paleozoic to Triassic magmatism of southwestern Gondwana, and the relationships with the volcanogenic events in coeval basins. *Journal of South American Earth Sciences*, *63*, 48–69.

Schlische, R. W. (1991). Half-graben basin filling models: New constraints on continental extensional basin development. *Basin Research*, *3*(3), 123–141.

Scholz, C. H., & Contreras, J. C. (1998). Mechanics of continental rift architecture. *Geology*, *26*(11), 967–970.

Scivetti, N., & Franzese, J. R. (2019). Late Triassic-late Jurassic subsidence analysis in Neuquén Basin central area. *Journal of South American Earth Sciences*, *94*, 102230.

Silvestro, J., & Zubiri, M. (2008). Convergencia oblicua: modelo estructural alternativo para la Dorsal Neuquina (39°S)-Neuquén. *Revista de la Asociación Geológica Argentina*, *63*(1), 49–64.

Spalletti, L. A., Arregui, C. D., Veiga, G. D., Leanza, H. A., Carbone, O., Danielli, J. C., & Vallés, J. M. (2011). La Formación Tordillo y equivalentes (Jurásico Tardío) en la Cuenca Neuquina. In H. A. Leanza, C. Arregui, O. Carbone, J. C. Daniela, & J. M. Vallés (Eds.), *Geología y Recursos Naturales de la Provincia del Neuquén. Relatorio del XVIII Congreso Geológico Argentino* (pp. 99–111). Asociación Geológica Argentina.

Spalletti, L. A., & Limarino, C. O. (2017). The Choiyoi magmatism in south western Gondwana: Implications for the end-permian mass extinction-a review. *Andean Geology*, *44*(3), 328–338.

Spalletti, L. A., & Piñol, F. C. (2005). From alluvial fan to playa: An upper Jurassic ephemeral fluvial system, Neuquén Basin, Argentina. *Gondwana Research*, *8*(3), 363–383.

Spalletti, L. A., Queralt, I., Matheos, S. D., Colombo, F., & Maggi, J. (2008). Sedimentary petrology and geochemistry of siliciclastic rocks from the upper Jurassic Tordillo formation (Neuquén Basin, western Argentina): Implications for provenance and tectonic setting. *Journal of South American Earth Sciences*, *25*(4), 440–463.

Spalletti, L. A., & Veiga, G. D. (2007). Variability of continental depositional systems during lowstand sedimentation: An example from the Kimmeridgian of the Neuquén Basin, Argentina. *Latin American Journal of Sedimentology and Basin Analysis*, *14*(2), 85–104.

Sruoga, P., Etcheverría, M., Cegarra, M., Rubinstein, N. A., & Mescua, J. F. (2011). Engranaje lateral entre las Formaciones Tordillo y Río Damas en la Cordillera Principal de Mendoza (34° 45′ S). *Actas XVIII Congreso Geológico Argentino*, 4–6.

Stipanicic, P. N. (1969). El avance en los conocimientos del Jurásico argentino a partir del esquema de Groeber. *Revista de la Asociación Geológica Argentina*, *24*(4), 367–388.

Stipanicic, P. N., & Rodrigo, F. (1970). El diastrofismo jurásico en Argentina y Chile. *Actas IV Jornadas Geológicas Argentinas*, *2*, 353–368.

Tapia, F., Muñoz, M., Farías, M., Charrier, R., & Astaburuaga, D. (2020). Middle Jurassic-late cretaceous paleogeography of the Western margin of the Neuquén Basin (34° 30′–36°S). In D. Kietzmann & A. Folguera (Eds.), *Opening and closure of the Neuquén Basin in the southern Andes* (pp. 269–301). Springer Earth System Sciences.

Tunbridge, I. P. (1981). Sandy high-energy flood sedimentation—Some criteria for recognition, with an example from the Devonian of SW England. *Sedimentary Geology*, *28*(2), 79–95.

Tunik, M., Folguera, A., Naipauer, M., Pimentel, M., & Ramos, V. A. (2010). Early uplift and orogenic deformation in the Neuquén Basin: constraints on the Andean uplift from U–Pb and Hf isotopic data of detrital zircons. *Tectonophysics*, *489*(1–4), 258–273.

Turnbridge, I. P. (1984). Facies model for a sandy ephemeral stream and clay playa complex; the middle Devonian Trentishoe formation of North Devon, UK. *Sedimentology*, *31*, 697–715.

Uliana, M. A., & Biddle, K. T. (1988). Mesozoic-Cenozoic paleogeographic and geodynamic evolution of southern South America. *Revista Brasileira de Geociencias*, *18*(2), 172–190.

Veiga, G. D., Howell, J. A., & Strömbäck, A. (2005). Anatomy of a mixed marine-non-marine lowstand wedge in a ramp setting. The record of a Barremian-Aptian complex relative sea-level

fall in the Central Neuquén Basin, Argentina. *Geological Society of London, Special Publications*, *252*(1), 139–162.

Vennari, V. V., Lescano, M., Naipauer, M., Aguirre-Urreta, B., Concheyro, A., Schaltegger, U., Armstrong, R., Pimentel, M., & Ramos, V. A. (2014). New constraints on the Jurassic–cretaceous boundary in the high Andes using high-precision U–Pb data. *Gondwana Research*, *26*(1), 374–385.

Vergani, G. D., Tankard, A. J., Belotti, H. J., & Welsink, H. J. (1995). Tectonic evolution and paleogeography of the Neuquen Basin, Argentina. In A. J. Tankard, R. Suárez, & H. J. Welsink (Eds.), *Petroleum basins of South America* (Vol. *62*, pp. 383–402). American Association of Petroleum Geologists Memoir.

Vergara, M., Levi, B., Nystrom, J., & Cancino, A. (1995). Jurassic and early cretaceous Island arc volcanism, extension, and subsidence in the coast range of Central Chile. *Geological Society of America Bulletin*, *107*, 1427–1440.

Vermeesch, P. (2018). IsoplotR: A free and open toolbox for geochronology. *Geoscience Frontiers*, *9*(5), 1479–1493.

Vermeesch, P. (2021). Maximum depositional age estimation revisited. *Geoscience Frontiers*, *12*(2), 843–850.

Vicente, J. C. (2005). Dynamic paleogeography of the Jurassic Andean basin: Pattern of transgression and localisation of main straits through the magmatic arc. *Revista de la Asociación Geológica Argentina*, *60*, 221–250.

Vicente, J. C. (2006). Dynamic paleogeography of the Jurassic Andean basin: Pattern of regression and general considerations on main features. *Revista de la Asociación Geológica Argentina*, *61*(3), 408–437.

Vicente, J. C., & Leanza, H. A. (2009). El frente de corrimiento andino al nivel de los cerros Penitentes y Visera (alta Cordillera de Mendoza): aspectos cronológicos y cartográficos. *Revista de la Asociación Geológica Argentina*, *65*(1), 97–110.

Walsh, J. J., & Watterson, J. (1989). Displacement gradients on fault surfaces. *Journal of Structural Geology*, *11*(3), 307–316.

Whitmeyer, S. J., Pyle, E. J., Pavlis, T. L., Swanger, W., & Roberts, L. (2019). Modern approaches to field data collection and mapping: Digital methods, crowdsourcing, and the future of statistical analyses. *Journal of Structural Geology*, *125*, 29–40.

Worthington, R. P., & Walsh, J. J. (2017). Timing, growth and structure of a reactivated basin-bounding fault. *Geological Society, London, Special Publications*, *439*(1), 511–531.

Wright, V. P. (1988). Paleokarsts and paleosols as indicators of paleoclimate and porosity evolution: A case study from the carboniferous of South Wales. In N. P. James & P. W. Choquette (Eds.), *Paleokarst* (pp. 329–341). Springer.

Zappettini, E., Méndez, V., & Zanettini, J. C. (1987). Metasedimentitas mesopaleozoicas en el noroeste de la Provincia del Neuquén. *Revista de la Asociación Geológica Argentina*, *42*(1–2), 206–207.

Zavala, C., Arcuri, M., Di Meglio, M., Zorzano, A., & Otharán, G. (2020). Jurassic uplift along the Huincul arch and its consequences in the stratigraphy of the Cuyo and Lotena groups. Neuquén Basin, Argentina. In D. Kietzmann & A. Folguera (Eds.), *Opening and closure of the Neuquén Basin in the southern Andes* (pp. 53–74). Springer Earth System Sciences.

Zavala, C., & Freije, H. (2002). *Cuñas clásticas jurásicas vinculadas a la Dorsal de Huincul. Un ejemplo del área de Picún Leufú, Cuenca Neuquina, Argentina* (p. 14). Actas V Congreso de exploración y desarrollo de Hidrocarburos.

Ziegler, P. A., & Cloetingh, S. (2004). Dynamic processes controlling evolution of rifted basins. *Earth-Science Reviews*, *64*(1–2), 1–50.

Zöllner, W., & Amos, A. J. (1973). *Descripción geológica de la hoja 32b, Chos Malal. Provincia del Neuquén*. Servicio Geológico Nacional.

SUPPORTING INFORMATION

Additional supporting information can be found online in the Supporting Information section at the end of this article.

How to cite this article: Acevedo, E., Fernández Paz, L., Encinas, A., Horton, B. K., Hernando, A., Valencia, V., & Folguera, A. (2023). Late Jurassic back-arc extension in the Neuquén Basin (37°S): Insights from structural, sedimentological and provenance analyses. *Basin Research*, *35*, 1012–1036. https://doi.org/10.1111/bre.12744